universität wien

MASTERARBEIT

Titel der Masterarbeit

„Analysis of the PI3K pathway in breast cancer“

verfasst von

Anna Buder BSc

angestrebter akademischer Grad

Master of Science (MSc)

Wien, 2015

Studienkennzahl lt. Studienblatt:	A 066830
Studienrichtung lt. Studienblatt:	Masterstudium Molekulare Mikrobiologie und Immunbiologie
Betreut von:	Assoc. Prof. Mag. Dr. Martin Filipits

Table of contents:

Abstract:

Purpose: To assess the prognostic and/or predictive value of phosphatidylinositide 3-kinase catalytic subunit alpha (*PIK3CA*) gene mutations, the downstream effectors of the PI3K/Akt/mTOR pathway, phospho-mTOR and phospho-S6RP, as well as clinical parameters on late distant recurrence (beyond 5 years after diagnosis and treatment) in a large cohort of postmenopausal, endocrine-responsive breast cancer patients.

Experimental Design: DNA was isolated from 527 formalin-fixed, paraffin-embedded tumor samples of postmenopausal endocrine-responsive breast cancers from patients included in the prospectively randomized trial ABCSG 6a who had received no further therapy after completed tamoxifen treatment or three years of extended therapy with anastrazole. For mutational analysis of the *PIK3CA* gene pyrosequencing was used. Expression of phospho-mTOR and phospho-S6RP was determined by immunohistochemistry on whole tumor tissue sections of patients of ABCSG trial 6a. Cox-models adjusted for clinical and pathological parameters were used to study distant recurrence-free survival (DRFS).

Results: Mutations in the *PIK3CA* gene were found in 42.4% of breast tumors but had neither prognostic nor predictive value. Interestingly, we observed a significant interaction between high phospho-mTOR expression as well as high progesterone receptor (PgR) expression and extended adjuvant endocrine treatment (P=0.03 and P=0.01, respectively). For patients classified as phospho-mTOR high or PgR high, a significant treatment effect was observed, with the hazard of a DRFS event being greater for the observation group compared to patients treated with extended endocrine therapy (P=0.02 and P=0.001, respectively). In contrast, no statistically significant effect of extended endocrine treatment was detected in the phospho-mTOR low or PgR low group (P=0.34 and P=0.71, respectively), indicating that phospho-mTOR low or PgR low patients derived little or no benefit from extended endocrine treatment.

Conclusion: *PIK3CA* mutations had no significant prognostic and/or predictive relevance in our cohort of breast cancer patients. Women with high phospho-mTOR expression or high PgR expression appear to benefit from extension of endocrine therapy after 5 years of treatment with tamoxifen, whereas patients with low phospho-mTOR expression or low PgR expression do not.

Zusammenfassung:

Studienziel: Studienziel war die Untersuchung der prognostischen und/oder prädiktiven Wertigkeit von Mutationen der katalytischen Untereinheit Alpha der Phosphatidylinositid 3-Kinase (*PIK3CA*), der Effektoren des PI3K/Akt/mTOR-Signalwegs, Phospho-mTOR und Phospho-S6RP, sowie klinischer Parameter bezüglich der späten Fernmetastasierung (über 5 Jahre nach der Diagnose und Behandlung) in einer großen Kohorte von postmenopausalen endokrin behandelbaren Brustkrebspatientinnen.

Methoden: DNA wurde aus 527 formalin-fixierten, paraffin-eingebetteten Tumorproben von postmenopausalen endokrin behandelbaren Brustkrebspatientinnen der prospektiv randomisierten Studie ABCSG 6a extrahiert. Diese Patientinnen erhielten entweder keine weitere Therapie nach abgeschlossener Tamoxifenbehandlung oder drei Jahre verlängerte Therapie mit Anastrazol. Zur *PIK3CA*-Mutationsanalyse wurde Pyrosequenzierung verwendet. Die Expression von Phospho-mTOR und Phospho-S6RP wurde immunohistochemisch an Tumorgewebsschnitten von Patientinnen der ABCSG 6a Studie bestimmt. Cox-Modelle, korrigiert nach klinischen und pathologischen Parametern, wurden angewendet um das fernmetastasenfreie Überleben (DRFS) zu untersuchen.

Ergebnisse: Mutationen im *PIK3CA* Gen wurden in 42.5 % der Brusttumore festgestellt, hatten jedoch weder prognostische noch prädiktive Aussagekraft. Interessanterweise beobachteten wir eine signifikante Wechselwirkung zwischen hoher Phospho-mTOR-Expression sowie hoher Progesteronrezeptor (PgR)-Expression und der verlängerten, adjuvanten, Hormontherapie (P=0.03 beziehungsweise P=0.01). Für Patientinnen, welche als stark Phospho-mTOR positiv oder stark PgR positiv eingestuft wurden, konnte eine signifikante Verlängerung des DRFS durch die verlängerte Hormontherapie nachgewiesen werden (P=0.02 beziehungsweise P=0.001). Im Gegensatz dazu wurde keine statistisch signifikante Verlängerung des DRFS durch die verlängerte endokrine Behandlung bei Patientinnen mit niedrigem Phospho-mTOR oder niedrigem PgR beobachtet (P=0.34 beziehungsweise P=0.71).

Fazit: *PIK3CA*-Mutationen hatten weder eine signifikante prognostische noch eine prädiktive Bedeutung in unserer Kohorte von Brustkrebspatientinnen. Frauen mit hoher Phospho-mTOR- oder hoher PgR-Expression im Tumor scheinen von einer Verlängerung der endokrinen Therapie nach 5 Jahren Behandlung mit Tamoxifen zu profitieren, wohingegen

Patientinnen mit niedriger Phospho-mTOR- oder niedriger PgR-Expression keinen Vorteil durch die verlängerte endokrine Therapie haben.

Introduction

1.1 Study background:

Breast cancer is the most frequently diagnosed cancer in women worldwide with approximately 1.7 million new cases every year (International Agency for Research on Cancer WHO 2013). In Austria, one woman among 13 will be diagnosed with breast cancer before reaching the age of 75 (Statistics Austria, as of 2011).

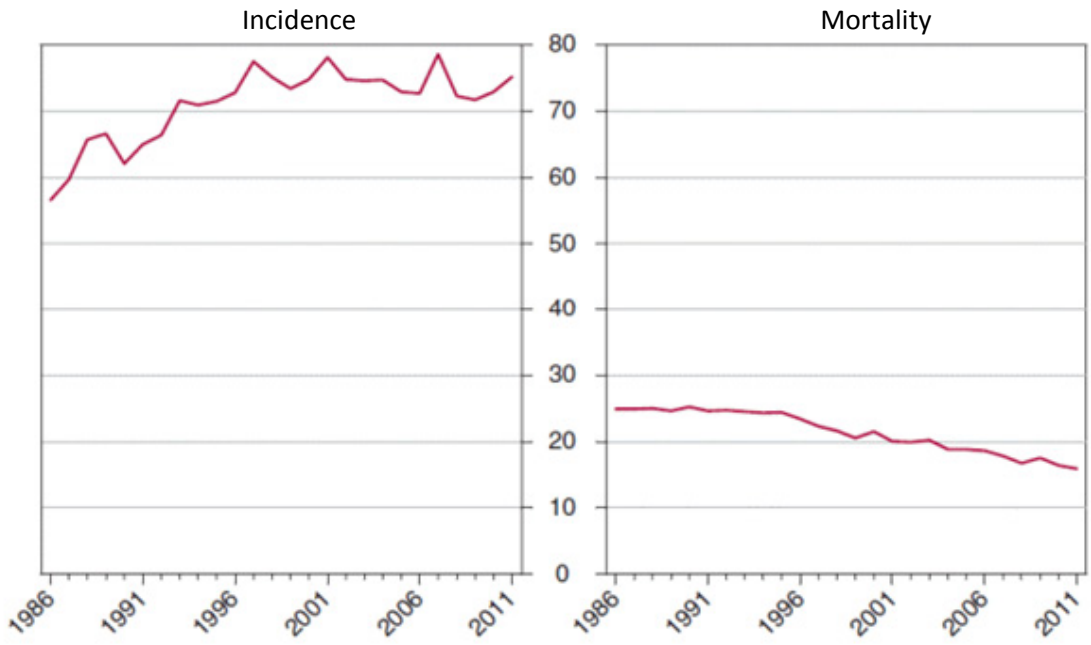

Figure 1: New cases of malignant neoplasms in women in Austria since 1986 (on the left) and the resulting mortality rate (on the right).STATISTIK AUSTRIA, Austrian Cancer Register and Causes of Mortality. (as of 17.10.2013) Compiled 25.10.2013

However, breast cancer does not represent a homogenous disease that allows consistent risk assessment and uniform strategies for molecular targeting of cellular points of attack. Thus it is necessary to detect individual tumor characteristics to predict its effects on the patient and to estimate its response to treatment. Clinical or biological characteristics of the tumor can be classified according to their informative value into two categories of markers; prognostic and predictive markers. While prognostic markers are clinical or biological characteristics that indicate the presumable outcome of the cancer disease independently of treatment and allow a certain risk evaluation of an untreated individual, predictive markers are indicators for the therapeutic outcome and are used to assess the benefit of certain therapies for specific

subpopulations of patients [1]. The detection of new molecular markers still remains important to allow a more accurate evaluation of individual risks and treatment options of each patient enabling a better adjustment of therapy.

1.2.1 Phosphatidylinositol 3-kinase (PI3K):

Phosphatidylinositol 3-kinases (PI3Ks) constitute a family of related, intracellular lipid kinases. They play an important role as signal transducers by the phosphorylation of the 3´hydroxyl group of phosphatidylinositol and phosphoinositides resulting in the activation of diverse signaling cascades.
Major functions of these activated signaling pathways include regulation of cellular proliferation and survival, alterations of the cell metabolism and growth [2][3].
The family of PI3Ks comprises three distinct classes of enzymes according to their substrate specificity and primary structure. Each enzyme class performs unique regulatory functions in the cellular signal transduction cascade.
Class I enzymes are heterodimers composed of a catalytic subunit (110-120kDa) which is associated with a regulatory subunit. They perform the phosphorylation from phosphatidylinositol-4, 5-biphosphate (PIP2) into phosphosphatidylinositol-3, 4, 5-triphosphate (PIP_3) in vivo and are sub-classified into class IA and IB according to structural differences [4][5].
The subclass IA comprises a p110 catalytic subunit and a p85 regulatory subunit both featuring several isoforms [3].
The three isoforms of the catalytic subunit; p110α, p110β and p110δ are encoded by the three genes *PIK3CA*, PIK3CB and PIK3CD respectively. Similarly the isoforms of the regulatory subunit p85 are encoded by three distinct genes (PIK3R1, PIK3R2 and PIK3R3). The isoforms p85α, p55α and p50α represent different splicing variants of the same gene, PIK3R1. PIK3R2 only encodes the isoform p85β and PIK3R3 expression yields the p55γ isoform [3][4].
Structurally p110α is comprised of five domains which are illustrated in Figure 2. The adaptor binding domain (ABD) at the N-terminus interacts with the regulatory subunit p85 and is followed by a Ras-binding domain (RBD) that allows binding and subsequent activation by the small GTPase Ras. In addition p110α features a C2 domain, a helical domain, also

referred to as phosphatidylinositol kinase homology (PIK) domain and a kinase catalytic domain [2][3].

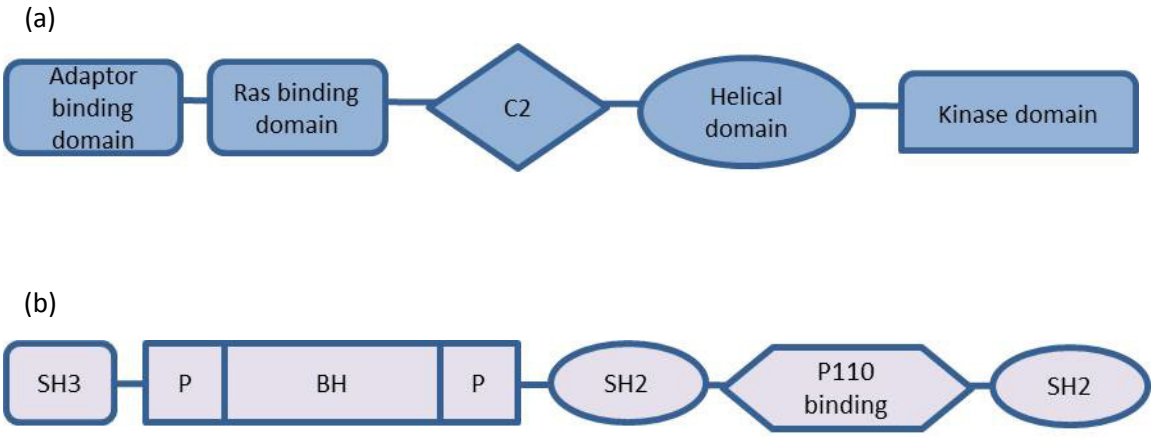

Figure 2: Scheme of the structural organization of the (a) p110α catalytic subunit and (b) p85 regulatory subunit (2)

1.2.2 PI3K-pathway alterations in breast cancer:

Mutations in phosphatidylinositol-3 kinase catalytic subunit alpha (PI3KCA) are very common in cancer patients and were detected in over 30% of solid tumors (Samuels & Ericson 2006). The phosphatidylinositol-3 kinase (PI3K) signaling pathway is critical for a number of fundamental cellular processes. However the major elements of the PI3K pathway are frequently mutated or amplified in various types of cancers. The PI3-kinase and its downstream pathway has therefore become subject of extensive research in the field of oncology.

1.2.3 Point mutations in the *PIK3CA* gene:

Numerous studies have confirmed that somatic mutations in the *PIK3CA* gene can be detected in a wide range of primary tumors including colorectal, gastric, brain and breast cancers as

well as in various cancer cell lines. In contrast they have not been reported for medulloblastomas and pancreatic cancers and are rare in lung adenocarcinomas [6]. Overall 1493 of the total 5838 breast cancer samples registered in the Cosmic database feature *PIK3CA* mutations, yielding a mutation rate of 26%. The highest frequencies of these mutations occur in hormone receptor positive and HER2 positive cancers [7]. Sabine et al. (2014) report a *PIK3CA* mutation rate of 40% in hormone receptor-positive luminal cancers (48). 95% of detected mutations were located in the helical (exon 9) and in the kinase (exon 20) domain. The ten most frequent *PIK3CA* mutations which together represent over 90% of mutations declared by the Cosmic database are listed in table 1. Interestingly the high frequency of the *PIK3CA* mutation E545K was almost solely detected in luminal A tumors and only very rarely in other breast cancer subtypes.

Mutation (CDS)	Mutation (Amino acid)	Frequency	Exon
c.1035T>A	p.N345K	46	Exon 4
c.1258T>C	p.C420R	21	Exon 7
c.1634A>G	p.E545G	18	Exon 9
c.1637A>G	p.Q546R	15	Exon 9
c.1634A>C	p.E545A	32	Exon 9
c.1633G>A	p.E545K	564	Exon 9
c.1624G>A	p.E542K	310	Exon 9
c.3140A>G	p.H1047R	1450	Exon 20
c.3140A>T	p.H1047L	153	Exon 20

Table 1: Overview of the most frequent point mutations in the *PIK3CA* gene. The nucleotide code for each mutation, the respective protein codes (CDS= Coding sequence) and the exons in which the mutations are located are indicated. The data originates from the Cosmic database (http://www.sanger.ac.uk/genetics/CGP/cosmic/)

In vitro studies with chicken embryo fibroblasts (CEF) show that mutations of the *PIK3CA* gene lead to a gain of enzymatic function. Cells harboring these mutations show a high

potential for the induction of oncogenic transformations and display elevated lipid-kinase activity. Enhanced enzymatic activity causes constitutive phosphorylation of Akt, p70 S6K and 4E-BP1 and therefore increases downstream signaling. All these potential mutants of *PIK3CA* constitute a hyper-active, growth-promoting enzyme that harbors major benefits compared to wild-type cells.

Overall, mutations were detected in the C2 domain, the helical domain and the kinase domain of the *PIK3CA* gene, suggesting that their effects on the function of p110α are accomplished by distinct molecular mechanisms. Mutations in the C2 domain facilitate binding and interaction with phospholipids at the cell membrane by augmenting the basic positive surface charge of this domain. In the helical domain, mutations mostly reside at the exposed surface of the domain; hence they could promote molecular interaction with other molecules or with the cellular membrane. As mutations in the kinase domain are clustered in close proximity to the activation loop they could shift the activation loop towards a permanently active position [9][10].

The consequences of *PIK3CA* mutations compared to wild-type *PIK3CA* and the resulting prognosis for the patients are still under debate with different studies reporting both, improved or deteriorated clinical outcomes. The major reason for these inconsistent conclusions could be the fact that breast cancer does not constitute a consistent pathophysiology. Firstly, the intrinsic tumor characteristics such as ER-positivity, HER2- positivity, or triple-negative condition, molecularly distinguish tumors with specific biological and clinical behaviors. The effect of *PIK3CA* mutations are also very likely to differ according to variations in the study cohort; (for example different hormonal status of patients). Finally, the domain and the exact location of the mutation in the *PIK3CA* gene could provide an additional parameter.

A comprehensive comparison of the most extensive breast cancer studies (12 studies covering 2587 breast cancer cases in total) published on PubMed in December 2011 reveals mutations in the kinase domain of the *PIK3CA* as a predominantly favorable predictive factor for OS (overall survival) and for responsiveness to hormonal therapy of postmenopausal, estrogen receptor-positive patients [11].

Moreover a recently conducted study by Sabine et al. (2014) demonstrated significant associations between *PIK3CA* mutations and favorable prognostic risk factors (HER2-negativity, low Ki-67 status, low tumor grade and size) in hormone-positive breast cancer patients. These correlations strongly indicate a connection to low-risk luminal breast cancer although no independent prognostic impact on DRFS could be shown [8].

1.2.4 Frequency of PIK3-Kinase Mutations in breast cancer:

The Cancer Genome Atlas Network (2012) conducted a broad mutational analysis of 507 breast tumors identifying 35 significantly mutated genes (SMG) from which the following three showed the highest mutation frequencies: TP53 (37%), *PIK3CA* (36%) and GATA3 (11%). However within the luminal A subtype most somatic mutations were detected in the *PIK3CA* gene (45%) (Figure 3). As shown in figure 3 *PIK3CA* mutations occur less frequently in luminal B (29%), Her2 enriched (39%) and basal-like (9%) tumors[7].

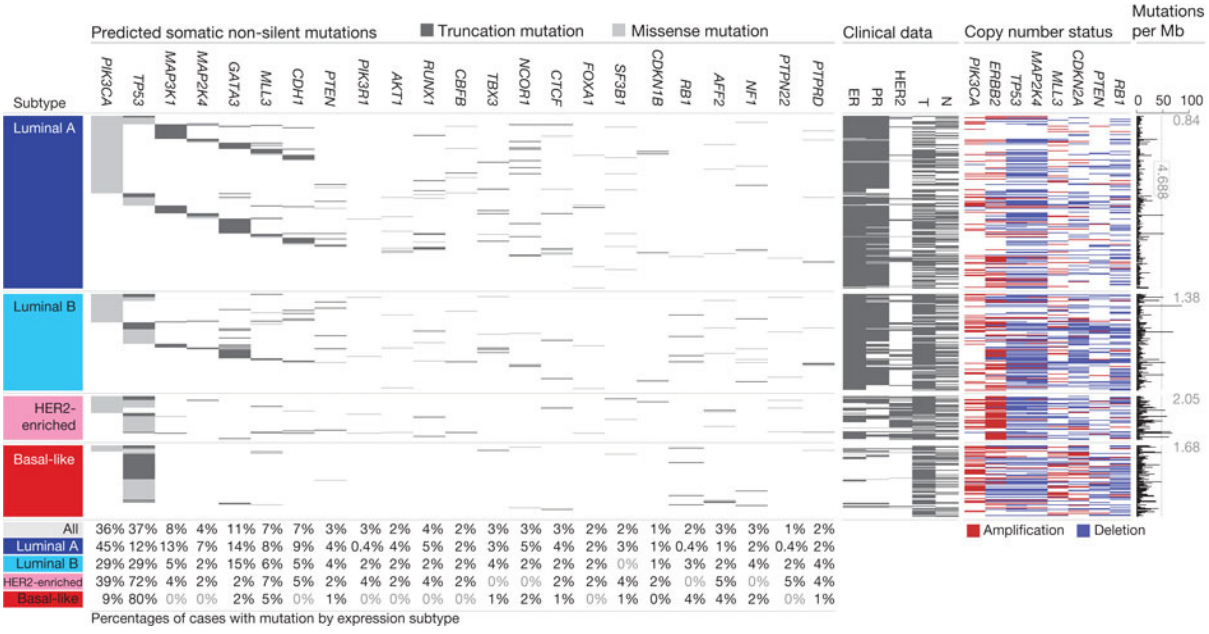

Figure 3: Overview of significantly mutated genes (SMG) in the four tumor subtypes and their respective genomic characteristics and clinical properties are shown [7]

1.2.5 Relevance of *PIK3CA* mutations for prognosis and therapy:

As mutations in the *PIK3CA* are very common in breast cancer their impact on therapy responsiveness is still subject of debate and was investigated in various studies. Although in many cases mutations have been considered as drivers for cancer evolution and therapy resistance they might also provide a promising target for drug therapy. Consequently the

identification of the mutational status of the *PIK3CA* gene could serve as predictive marker to guide adjusted medical treatment.

A current example for the role of particular mutations as predictive biomarker for better therapeutic adaptations comes from lung cancer research. In the case of non-small lung carcinomas EGFR mutations constitute a predictive biomarker whose presence correlates significantly with an increase in progression-free survival (PFS) under administration of EGFR–tyrosine kinase inhibitors (TKIs) [12].

A recent study showed that the incidence of *PIK3CA* mutations does not present an independent risk factor in ER-positive breast cancer but is associated with several favorable prognostic factors including PgR positivity, low tumor grade or lymph node negativity. In addition, these mutations occur more frequently in luminal A compared to luminal B tumors. All these findings suggest a positive correlation between *PIK3CA* mutations and a more favorable clinical prognosis [8]. Interestingly, a study by Campbell et al. (2001) showed that the PI3-kinase pathway enhances estrogen-stimulated activity of ERα and also confers its activation in an ER independent manner. Moreover in vitro experiments indicated that tamoxifen resistance was caused by enhanced Bcl-2 expression mediated by Akt [13]. Additionally, the deliberate deregulation of the PI3K-pathway through knockdown of PTEN or overexpression of oncogenes (HER2, AIB1) which activate PI3K/AKT signaling resulted in resistance to tamoxifen. Subsequent treatment with inhibitors of the RTK pathway (Gefitinib, AKTi, BEZ235, or AEW541) abrogated antiestrogen resistance in different cancer cell lines [14][15].

At present various inhibitory molecules targeting the PI3K pathway are tested in clinical trials of breast cancer treatment [14]. These molecules include panPI3K inhibitors, PI3Kα inhibitors, and dual PI3K/mTOR inhibitors [16].

1.3.1 PI3K/Akt/mTOR pathway:

As already mentioned subclass IA PI3-kinases are activated by receptor tyrosine kinases (RTKs). RTKs exhibit a broad spectrum of cell surface receptors that are activated by a variety of extracellular signaling proteins. Examples for activating ligands include epidermal growth factor (EGF), platelet-derived growth factor (PGF), fibroblast growth factor (FGF) hepatocyte growth factor (HGF), insulin, insulin-like growth factor-1 (IGF1), vascular endothelial growth factor (VEGF) and many more [17].

Upon ligand binding autophosphorylation (dimerization and subsequent cross-phosphorylation) of several tyrosines of cytosolic receptor chains takes place. Phosphorylated tyrosines in the kinase domain serve as docking sites for the regulatory subunit (p85) of the PI3-kinase. The p110 binding domain of p85 is flanked by SH2 domains (figure 2). These SH2 domains mediate PI3-kinase activation by binding to the tyrosine residues of activated RTK [17][2].

The active PI3-kinase generates phosphosphatidylinositol-3, 4, 5- triphosphate (PIP_3) by phosphorylation of the 3-position of the inositol ring of phosphatidylinositol-4, 5-biphosphate (PIP2) [5]. This reaction can be reversed by dephosphorylation of PIP3 through the tumor suppressor PTEN. Consequently PTEN controls cellular levels of PIP3 thus inhibiting the activation of downstream signaling molecules (Simpson &Parsons, 2001).

PIP3 is essential for the recruitment of the serine/threonine kinase Akt/PKB to the plasma-membrane. Akt features a pleckstrin homology (PH) domain which enables this kinase to bind to the phospholipid PIP3 and to undergo a conformational change that allows its phosphorylation by phospho-inositide dependent kinase-1 (PDK1) on Thr308 within the activation T-loop [18]. However, full activation of Akt requires a second phosphorylation by the rapamycin insensitive companion of mTOR (Rictor), a member of the mammalian target of rapamycin 2 (mTORC2). Rictor phosphorylates Akt at Ser473 located in the hydrophobic motif of the carboxyl terminal domain [19].In the active state Akt functions as an important mediator of signal transduction processes that promotes cell survival and growth though the phosphorylation of a variety of target proteins at the plasma membrane as well as in the cytosol and in the nucleus. Principal targets include the Forkhead box family of transcription factors (FOXO) or the pro-apoptotic protein Bad (Bcl-2-associated death promoter protein) which is converted into an inactive state upon phosphorylation in order to support cell survival [17][20]. Moreover cell growth can be supported by Akt via indirect activation of the mammalian target of rapamycin complex 1 (mTORC1) which promotes protein translation and cell growth and functions as a key regulator of metabolism and autophagy [21][17][22][23].

The mTORC1 is kept in an inactive state until its negative regulator, tuberous sclerosis complex 2 (TSC2), is inactivated by Akt via phosphorylation [24]. Inactive TSC2 is incapacitated to maintain the small Ras-related GTPase (Rheb) in an inactive GDP-bound state. This enables Rheb to directly interact and activate mTORC1 [22].

1.3.2 Mammalian target of rapamycin (mTOR) complex formation:

The mammalian target of rapamycin (mTOR) is a 289kDa protein that was named with reference to its homologs in *Saccharomyces cerevisiae*, TOR1 and TOR2 and is likewise a target of rapamycin [25][26][27]. Furthermore mTOR is a serine/threonine kinase and represents a member of the phosphatidylinositol 3-kinase-related kinases (PIKK).
Principally, mTOR forms the catalytic subunit of the two structurally distinct multiprotein complexes mTOR complex 1 (mTORC1) and mTOR complex 2 (mTORC2).
Besides different protein composition of each of the mTOR complexes a major difference is entailed in the sensitivity to the bacterial macrolide rapamycin. Correspondingly, the distinct effects of rapamycin on the relative protein complexes mTORC1 are characteristically referred to as rapamycin-sensitive complex and mTORC2 as rapamycin-insensitive complex [28].
The protein composition of mTORC1 includes 5 components:

- mTOR
- mTOR regulatory associated protein of mTOR (Raptor)
- proline-rich AKT substrate 40 kDa (PRAS40)
- mammalian lethal with Sec13 protein 8 (mLST8)
- DEP-domain-containing mTOR interacting protein (DEPTOR)

The binding of the scaffold protein Raptor to mTOR is critical for the phosphorylation of the downstream targets of mTOR, 4E-BP I and S6K1 [29].
Negative regulation of mTORC1 is mediated by forming a complex with DEPTOR but also by PRAS40 which inhibits substrate binding to raptor and to the protein complex [30][31][32][33]. The phosphorylation of these inhibitory proteins by active mTORC1 promotes their release from the protein complex and allows unhindered mTORC1 signaling processes [32][33]. DEPTOR additionally inhibits the activity of mTORC2 [33].
The exact role of mLST8 has not been fully clarified as in vivo experiments showed that its presence is required only for the function of mTORC2 but not mTORC1 [34].
The formation of mTORC2 comprises 6 protein components [22]:

- mTOR
- rapamycin insensitive companion of mTOR (Rictor)
- mammalian stress-activated protein kinase interacting protein (mSIN1)
- protein observed with rictor-1 (Protor-1)

- mammalian lethal with Sec13 protein 8 (mLST8)
- DEP-domain-containing mTOR interacting protein (DEPTOR)

The binding of the key components Raptor and Rictor to mTOR happens in a mutually exclusive manner. Rictor plays a pivotal role for the phosphorylation of Akt and the regulation of the actin cytoskeleton through PKCα phosphorylation. This complex component is not directly inhibited by the immunosuppressant rapamycin [35][36]. Additionally a codependency between Rictor and mSIN1 for the assembly of mTORC2 was shown. mSIN1 occurs in different isoforms leading to several particular mTORC2s which were proposed to catalyze phosphorylation of Akt as a consequence of different upstream signals [37][20].

1.3.3 Downstream targets of mTORC1:

As described above the mTORC1 can be activated by growth factors via the PI3K/Akt pathway. Principal downstream operators of mTOR such as S6-kinase 1(S6K1), 4E-BP and eIF4B execute important functions as effectors in mRNA translation.

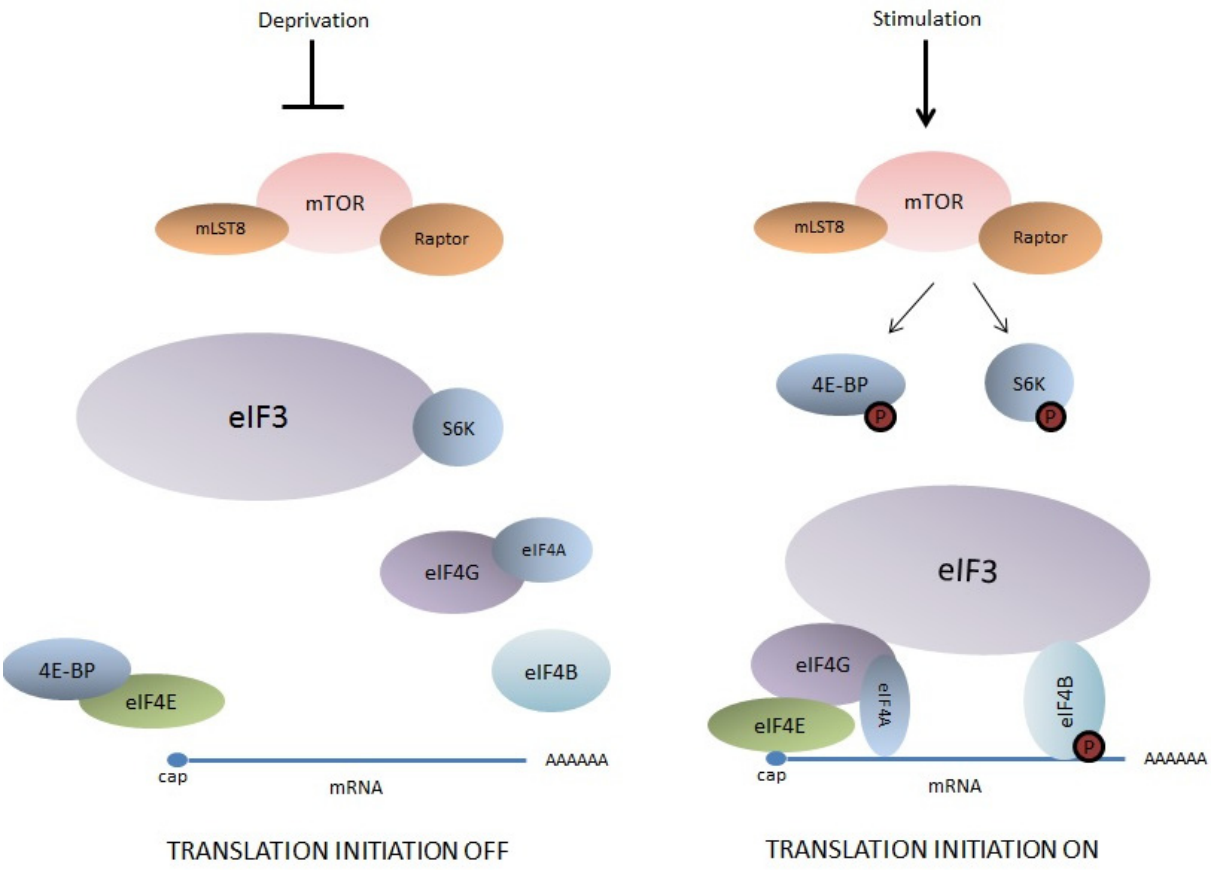

Figure 4: Translational control by downstream effectors of mTORC1, 4E-BP1 and S6-kinase 1 [38].

First of all the potential of mTORC1 to regulate protein synthesis is based on its ability to control ribosome binding to the 5´end (m7GpppN) of mRNAs. Regulation of this "rate-limiting step" in cap dependent translation is carried out indirectly by phosphorylation and subsequent inactivation of the translational repressor protein 4E-BP1. In its phosphorylated form this protein competes with the large ribosomal scaffolding protein eIF4G for binding to the eukaryotic initiation factor eIF4E and thereby inhibits the assembly of the ribosome recruitment machinery [39].

Phosphorylation of 4E-BP1 by mTOR is conducted at several sites in a hierarchical order beginning with Thr 37 and Thr 46 which enables further phosphorylation at Thr 70 and Ser 65. The dissociation of 4E-BP1 from the cap binding protein requires phosphorylation at each of the four sites [40][41][42][43]. Another important target of mTOR, S6-kinase 1, remains attached to eukaryotic initiation factor 3 (eIF3) unless mTOR is activated in response to various growth factors and nutrients (see above). Phosphorylation at T389 in the hydrophobic

motif by Raptor from the mTORC1 causes the release of eIF3 from S6K1 and subsequent binding of the kinase to phospho-inositide-dependent kinase 1 (PDK1) [44]. Further phosphorylation within the catalytic activation loop at T229 is performed by PDK1 which results in full activation of S6K1. Ultimately the active enzyme catalyzes the phosphorylation of various proteins including ribosomal S6 protein (S6) and eIF4B which are both associated with translation [38].

S6 is part of the 40S ribosomal subunit and plays a major role in the translational efficiency of mRNAs that feature a terminal oligopyrimidine tract (TOP). This 5´TOP sequence only comprises 4-14 nucleotides which are directly preceding the 5´cap sequence.

Characteristically this particular structure is exhibited by mRNAs encoding components of the ribosomal machinery such as, ribosomal proteins and elongation factors [44]. Translation of these mRNAs seems to follow an "all-or-non" phenomenon meaning that they are subjected to selective repression causing inefficient translation unless they enter an active state in which they are translated at nearly maximal rates. The fact that the initiation of this active high-level protein synthesis occurs simultaneously with the phosphorylation of the ribosomal protein S6 and that both incidents diminish under the impact of rapamycin indicates that ribosomes with high proportions of phosphorylated S6 show elevated translational affinity for TOP mRNAs [45].

However a study with mice deficient for S6-kinase suggests that S6 phosphorylation is linked to the MAPK pathway as neither S6 phosphorylation nor alterations in the translation of TOP mRNAs could be observed in the absence of S6-kinase. Nevertheless the frequency of growth defects and perinatal lethality increased in mice lacking S6-kinase [46].

1.4.1 Breast cancer subclasses:

In breast cancer three major molecular cancer subtypes; luminal, HER2-enriched and "basal-like" are differentiated.

The luminal subtype is further sub-classified into a luminal A and a luminal B cluster [47]. Evidence for this tumor classification was provided by gene expression profiling studies revealing distinct molecular portraits for different clusters of breast tumors [48][49].

The term "hormone-sensitive (or "hormone-dependent") breast cancer refers to the expression of hormone receptors by cancer cells which usually correlates with a certain dependence of tumor growth on hormonal stimulation. Hormone receptor positivity is most prevalent among

breast cancer with 2 out of 3 tumors expressing estrogen receptor (ER) and/or progesterone receptor (PgR) [50].

Although the luminal subtypes share the clinical designation of "ER positive" they may exhibit significantly different gene expression patterns. Luminal A tumors show high expression of the ERα gene together with other luminal specific genes while only low expression of this subset of genes is found in luminal B tumors [49]. The clinicopathological definition of the luminal A phenotype is based on hormone receptor positivity, the absence of HER2 (human epidermal growth factor receptor 2) and low expression of the nuclear protein Ki-67 [47].

The luminal B subtype which features higher expression of proliferation-related genes occurs in two particular phenotypes: "Luminal B-like (HER2 negative)" and "luminal B-like (HER2 positive)" [49][47].

Both, HER2-enriched and "basal-like" tumors are ER and PgR negative. As the term suggests, the HER2-enriched subtype is defined by high expression of genes of the ERBB2 amplicon. Finally the "basal-like subtype" represents a highly heterogeneous subtype which implies high expression of keratin 5 and 17, laminin and fatty acid binding protein 7. Approximately 80% of cases of the "basal-like" subtype correspond with the clinicopathological defined surrogate "triple negative" which lacks expression of all three receptors; ER, PgR, HER2 [47][49][51].

Each subtype maintains individual prognostic value which allows an estimation of the risk for cancer relapse, metastases and death.

1.4.2 Estimated risks of breast cancer subgroups:

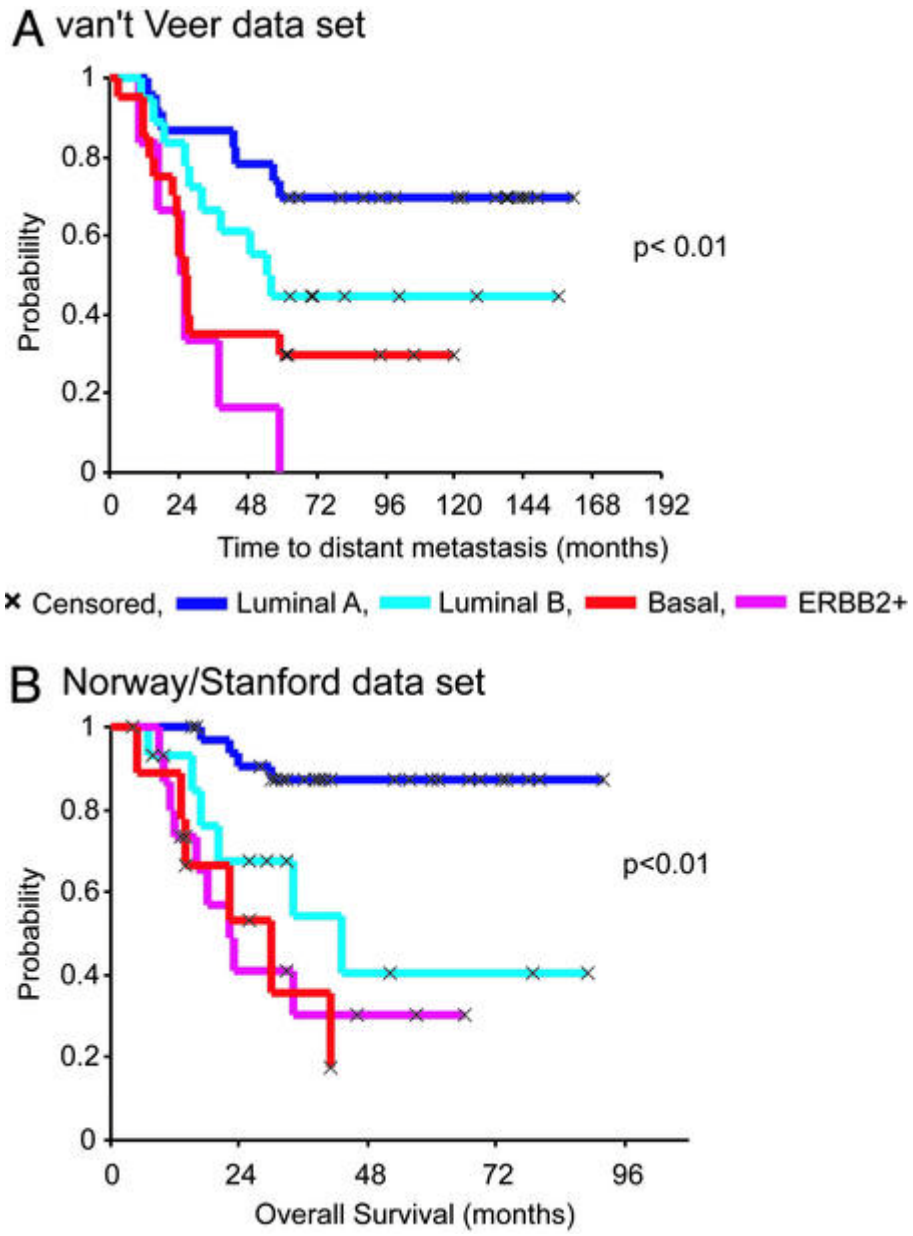

Figure 5: Kaplan–Meier analysis of disease outcome according to the molecular subtype in two patient cohorts. (*A*) Time to development of distant metastasis in the 97 sporadic cases from van't Veer *et al*. (*B*) Overall survival for 72 patients with locally advanced breast cancer in the Norway cohort [52].

Recurrence risk varies between the intrinsic subtypes and throughout the follow-up time. The mortality rate and the incidence of distant metastases and local recurrences for luminal A cancers is significantly lower compared to other breast cancer subtypes. Both, mortality rate and risk for distant metastases do not differ significantly between individual (HER2 positive/negative) subtypes of luminal B tumors and lie below those of HER2-enriched and triple-negative patients. Basal-like tumors especially if they are negative for all three receptors, anticipate the worst prognosis and the highest recurrence risk [53].

1.5.1 Hormone receptor-positive breast cancer therapy:

Over two thirds of breast cancers express ER and/or progesterone receptor (PgR) [54]. Hormone receptor-positive patients are candidates for treatment with drugs that specifically interfere with ER signaling. These "endocrine therapies" are often used alone or together with chemotherapy in high risk patients. Interference of ER signaling is targeted by either of two basic mechanisms [14].

Selective estrogen receptor modulators (SERMs) antagonize estrogen receptors and thereby prevent ligand-receptor binding. Examples for approved SERMs are tamoxifen for the treatment of early-breast cancer and toremifen for advanced (metastatic) breast cancer treatment [55].

In contrast, aromatase inhibitors block the final step of estrogen biosynthesis through the inhibition of the conversion of androgens (C_{19} steroids) into estrogens (C_{18} steroids) by the aromatase. Aromatase inhibitors are only recommended to postmenopausal patients as estrogen is no longer produced in ovaries but only decreased amounts are synthesized in peripheral tissues. Two types of aromatase inhibitors; type I and type II are approved for breast cancer treatment:

Type I inhibitors mimic the steroidal structure of androgens and irreversibly block the substrate-binding site of the aromatase enzyme. Examples of this type of treatment include formestane and exemestane.

Type II inhibitors like, for example anastrazole or letrozole compete for binding to the aromatase thereby preventing estrogen synthesis [56].

Meta-analysis of diverse breast cancer trials showed that adjuvant treatment with tamoxifen reduces the risk of recurrence over all time periods by 39%. During the first four years of treatment the recurrence risk can be reduced by approximately 50% and a reduction by

approximately a third can be achieved during the following five years. Only after a time period of ten years recurrence rates between tamoxifen treatment and control groups were concordant.

Furthermore several trials have been published recently which analyze the advantages of extended endocrine therapy after 5 years tamoxifen treatment for further reduction of the risk for cancer recurrence at longer time periods after initial diagnosis and treatment [57]. According to these analyses the treatment extension of tamoxifen for an additional 5 years is not recommended, whereas extended aromatase inhibitor is only recommended to the postmenopausal patients who had completed 5 years tamoxifen, and the aromatase inhibitor treatment duration should not exceed 5 years [57].

As the optimal timing and duration of extended adjuvant therapy after 5 years of endocrine treatment is currently unknown, there is an urgent need to identify the subpopulation that is likely to benefit from an extended and/or a molecular targeted strategy.

Administration of the aromatase inhibitor anastrazole for 3 years as extended adjuvant therapy after 5 years of tamoxifen treatment significantly reduced the risk of recurrence during a median follow-up of 62.3 months [58]. Furthermore studies in which patients switched after 2-3 years of adjuvant tamoxifen therapy to anastrazole treatment report lower recurrence risks and increased disease-free survival (DFS) rates [59].

Furthermore phase III trials evaluating the benefits of endocrine therapy extension with tamoxifen have been conducted (12). The ATLAS trial which included 13000 patients worldwide compared the cancer recurrence risks and cancer related deaths between a study group of patients who terminated treatment after five years of tamoxifen and another group who extended tamoxifen treatment for 5 more years resulting in a total of 10 years of tamoxifen therapy. Strikingly there was not only a slight risk reduction within the years 5-9 but after termination of therapy at 10 years a relative risk reduction of 25% and an absolute risk reduction of 3,7% was achieved at 15 years of follow-up(12).

To optimize the prognostication and prediction of late cancer recurrence or adjuvant chemotherapy benefit of individual patients various multigene assays have been developed and applied in different studies. The multigenomic tests EndoPredict (EP), the intrinsic subtype test (PAM50) (Prosigna) and HOXB13/IL17BR (part of the Breast Cancer index (BCI)) are based on reverse transcriptase-polymerase chain reactions (RT-PCR) and allow the calculation of scores that provide prognostic information which extends ER status based patient evaluations. These scores also represent an important contribution to the

comprehension of late recurrence risk and are very promising options for the identifications of low-risk subgroups among ER-positive breast cancer patients for which therapy extension would provide only little benefit [60].

1.5.2 Tamoxifen treatment-limits of protective effects:

Adjuvant treatment with tamoxifen significantly reduced the recurrence risk over all time periods by 39% [54]. Statistics show that the risk of death from ER-positive breast cancer 15 years after the administration of tamoxifen is three times higher than it was 5 years after the treatment started (Early Breast Cancer Trialists' Collaborative Group (EBCTCG 2005)). Whereas ER-negative tumors typically develop metastases within 5 years of initial diagnosis and treatment, ER-positive breast cancers show relatively stable annual recurrence rates after the first 5 years (Figure 6). Additionally ER-positive breast cancer patients under an age of 40 years face an approximately 2-fold increased hazard of breast cancer specific mortality (BCSM) than older patients.

Despite up to five years endocrine therapy many women with ER-positive tumors will relapse and die from breast cancer at 5-10 years after diagnosis. Strikingly during this time period the annual breast cancer specific mortality rate for ER-positive breast cancer exceeds the corresponding ER-negative rate (Figure 6) [57].

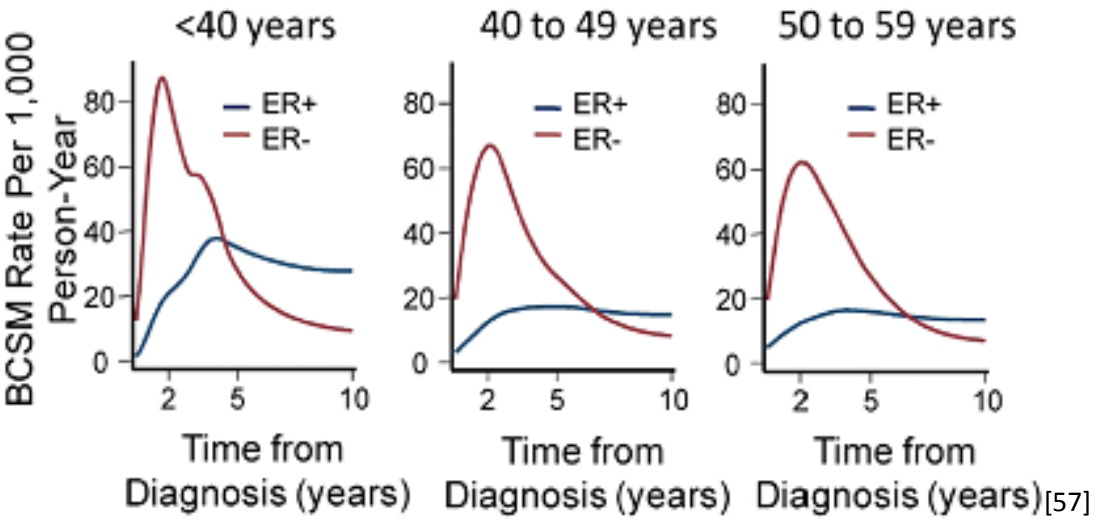

[57]

Figure 6: Estimated annual risk for breast cancer specific mortality (BCSM) for positive and negative ER-status is time-dependent. Different age groups show distinct courses of BCSM . Risk rates were reported per 1000 patients per year [57].

Several trails aiming risk reduction, especially at 5-10 years after diagnosis tested extension of endocrine therapy after 5 years of tamoxifen treatment [57]. The major challenge is to identify patients who face an increased risk and would therefore benefit the most from therapy extension. However distinct molecular subpopulations are undetermined although they feature increased risk of breast cancer specific mortality in advanced time periods of initial diagnosis and treatment (5-10 years). In order to optimize timing and duration of extended adjuvant therapy following 5 years of endocrine treatment a finer classification within the luminal patients cohort is required and would help to tailor a more targeted molecular treatment strategy for each patient [60].

Material & Methods

2.1 Study population:

The present investigation is part of the ABCSG translational research program (abcsg.research). All patients included in this study had participated in the large phase III trial ABCSG 6a. This study is an extension of the randomized phase III Trial 6 of the Austrian Breast and Colorectal Cancer Study Group (ABCSG) [61] [58].
ABCSG 6 compared tamoxifen alone for 5 years with tamoxifen for 5 years in combination with aminoglutethimide for the first 2 years of treatment in postmenopausal women. In this study no differences between the two treatment regimens were observed for 5 years [61]. ABCSG Trial 6a included study participants of ABCSG Trial 6 who were disease-free after five years of adjuvant treatment. These patients (n=856) were randomly assigned to be treated with the aromatase inhibitor anastrazole for 3 years starting within 6 weeks after the end of ABCSG Trial 6 or to receive no further treatment. ABCSG Trial 6a showed a benefit for patients who were treated with anastrazole. In this study, tissue samples of the primary tumor from 546 patients who had fully completed ABCSG Trial 6a could be used for mutational and immunohistochemical analyses of the PI3-kinase-pathway.

2.2 DNA extraction:

DNA was extracted from formalin-fixed, paraffin-embedded (FFPE) breast cancer samples. Of each patient sample two sections of five µm were used for the extraction of genomic DNA by employing the QIAamp® DNA FFPE Tissue Kit (Qiagen, Hilden, Germany) according to the manufacturer's protocol. This kit is designed for rapid purification of genomic DNA from FFPE tissue sections resulting in pure DNA which is suitable for PCR and further applications. Removal of paraffin was achieved by dissolving the tissue sections in xylene followed by purification with ethanol and precipitation of tissue material after centrifugation. The optimized buffer system allowed direct cell lysis and selective binding of DNA to the silica-based membrane of the QIAamp MinElute® columns. Digestion by proteinase K was performed at 56 °C for two hours followed by further digestion at 90 °C for one hour. Several centrifugation steps removed contaminants and enzyme inhibitors and purified, concentrated DNA could be eluted (Qiagen, 2010). DNA was eluted in 40 µl of Elution Buffer (Qiagen, Hilden, Germany).

Chemicals	Description
Buffer ATL	Tissue lysis buffer
Buffer AL	Lysis buffer
Buffer AW1	Supplied as a concentrate that had to be diluted with 25 ml 96 - 100 % ethanol
Buffer AW2	Supplied as a concentrate that had to be diluted with 30 ml 96 - 100 % ethanol
Proteinase K	Ready to use in a specially formulated storage buffer
Buffer ATE	Elution buffer

Table 2: Solutions supplied with the QIAamp® DNA FFPE Tissue Kit

Further chemicals required for the DNA extraction were xylene and ethanol (96 - 100 %). Also QIAamp MinElute® columns and collection tubes (2 ml) were included in the kit content.

Procedure:

1. Paraffin removal:
   - sections were dissolved in 1 ml xylene and paraffin was removed after centrifugation
   - precipitated tissue (pellet) was then dissolved in 1 ml ethanol and after centrifugation paraffin and xylene residues were removed

2. Cell lysis:
   - 180 µl Buffer ATL and 20 µl proteinase K were added successively and mixed by vortexing
   - samples were incubated at 56 °C for 2 h followed by incubation at 90 °C for 1 h to reverse formalin crosslinking of nucleic acids
   - to attain a homogenous solution 200 µl ethanol (100 %) and 200 µl Buffer AL were added and mixed by vortexing

3. DNA binding
    - the whole product was pipetted into the QIAamp MinElute® column placed in a 2 ml collection tube
    - after centrifugation for 1 min at 6000 g the flow-through and the collection tube was discarded (the QIAamp MinElute® column was placed in a new collection tube)

4. Washing
    - 500 µl Buffer AW1 were added
    - the sample was centrifuged for 1 min at 6000 g
    - the flow-through and the collection tube was discarded
    - the QIAamp MinElute® column was placed in a new collection tube
    - 500 µl Buffer AW2 were added
    - the sample was centrifuged for 1 min at 6000 g
    - the flow-through and the collection tube was discarded (the QIAamp MinElute® column was placed in a new collection tube)

5. Elution
    - 40 µl Buffer ATE were pipetted directly onto the membrane of the QIAamp MinElute® column
    - the sample was incubated approximately 1 min at room temperature
    - the sample was centrifuged at full speed (20,000 g)

The DNA extraction yielded a product of 40 µl DNA solution ready to use.

The concentration was quantified by utilization of a Nanodrop 1000 spectrophotometer (Peqlab, Biotechnologie GmbH, Polling, Austria). As the attained concentrations were highly variable all samples were diluted to a final concentration of 2 ng/µl of DNA in order to perform PCR with an optimal amount of 10 ng of template DNA.

2.3.1 Polymerase Chain Reaction (PCR)

In order to perform Pyrosequencing® for the detection of point mutations in four exons of the *PIK3CA* gene, enzymatic amplification of the isolated DNA via polymerase chain reaction (PCR) had to be conducted. Additionally the DNA strand serving as template DNA during pyrosequencing had to be hybridized with a biotin marker. This hybridization could be induced by the use of biotinylated primers in the PCR employing the PyroMark PCR Kit (Qiagen, Hilden, Germany)

2.3.2 Primers

All pairs of primers used for the amplification of DNA, their respective nucleotide sequences and the sizes of the relative amplicons are listed in table 3.
Each set of primers composed of a forward and a reverse primer encased the relative sequence of interest and one of the primers was biotinylated to allow later Pyrosequencing®. The nucleotide sequences of the primer pairs for specific amplification of domains of interest in exon 20 and 9 of the *PIK3CA* gene were used as described in previous publications (Table 3). Primers used for the sequencing of exon 4 and 7 were designed using PyroMark Assay Design Software 2.0 (Version 2.0.1.15).

Primer	*PIK3CA*	Nucleotide Sequence 5'→ 3'	Size (bp)	Reference
PIK3CA 20_Fwd	Exon 20	[biotin]-CAAGAGGCTTTGGAGTATTTCA	74	Nosho et al. 2008
PIK3CA 20_Rev		CAATCCATTTTTGTTGTCCA		
PIK3CA 9_Fwd	Exon 9	[biotin]-AACAGCTCAAAGCAATTTCTACACG	81	Nosho et al. 2008
PIK3CA 9_Rev		ACCTGTGACTCCATAGAAAATCTTT		
PIK3CA 7_Fwd	Exon 7	[biotin]-AATTTTCCTTTTGGGGAAGA	121	
PIK3CA 7_Rev		CAAACAAGTTTATATTTCCCCATGC		
PIK3CA 4_Fwd	Exon 4	ACGCATTTCCACAGCTACACCA	155	
PIK3CA 4_Rev		[biotin]-AAGCATCAGCATTTGACTTTACCT		

Table 3: Primers and their respective characteristics used for PCR

2.3.3 Reagents and Solutions

All reagents used for PCR were taken from the PyroMark PCR Kit (QIAGEN) and are listed below.

- PyroMark PCR Master Mix (2x)
  Contains HotStarTaq DNA Polymerase and PyroMark Reaction Buffer (comprising 1.5 mM $MgCl_2$ and dNTPs)
- CoralLoad® Concentrate (10x)
  Contains gel loading reagent, orange dye and red dye
- RNase-Free Water

The reaction composition and the mixing ration for PCR are described in table 4. Each run comprised a negative template control (NTC) for which the fraction of DNA was replaced by RNase-free water.
This reaction set up allowed exponential amplification of the template DNA as well as its biotinylation for the following Pyrosequencing® procedure.

Components	Volumes
PyroMark PCR Master Mix (2x)	12.5 µl
CoralLoad® Concentrate (10x)	2.5 µl
RNase-free water	2.5 µl
Primer	2.5 µl
Template DNA (2ng/µl) /RNase-free water	5.0 µl
Total Reaction Volume	25.0 µl

Table 4: Pipetting scheme for PCR preparation

2.3.4 Procedure

The capacity of the thermal cycler (C1000 Thermal Cycler, BioRad, California) allowed a maximum of 96 samples per run. To facilitate the procedure, a mastermix containing all PCR reagents without the template DNA was prepared. In the case of 96 simultaneous PCR reactions the mastermix was prepared for 100 samples to account for pipetting losses.
After addition of template DNA or RNase-free water for NTC the samples were briefly centrifuged and transferred into the thermal cycler and the PCR program was started.
The PCR conditions for amplification of Exon 20; 9 and 4 were identical and are described in table 5.

Cycles	PCR step	Temperature	Time
1	Initial activation step	95 °C	15 min
45	Denaturation	94 °C	30 sec
	Annealing	60 °C	30 sec
	Extension	72 °C	30 sec
1	Final extension	72 °C	10 min

Table 5: PCR conditions for primers 20, 9 and 4

The PCR conditions for amplification of Exon 7 are described in table 6.

Cycles	PCR step	Temperature	Time
1	Initial activation step	95 °C	15 min
45	Denaturation	94 °C	30 sec
	Annealing	56 °C	30 sec
	Extension	72 °C	30 sec
1	Final extension	72 °C	10 min

Table 6: PCR conditions for primer 7

After the reaction had been completed, the samples were directly processed or stored at -20 °C until further procedures were performed.

2.4.1 Agarose Gel Electrophoresis

To confirm successful amplifications of requested DNA sequences the PCR products were subjected to electrophoresis in an agarose gel (2 %).

2.4.2. Reagents and Solutions

Chemicals	Descriptions	Formula	Producer
Tris ultra pure	Tris-(hydroxymethyl)-aminomethane (≥ 99, 97 % p.a.)	C4H11NO3	Biomol GmbH
BoricAcid		H3BO3	BioRad
EDTA disodiumsaltdihdrate	Ethylenediaminotetraacetic acid disodium salt dihydrate (p.a. 99-101 %)	C10H14N2Na2O8 · 2H2O	Sigma-Aldrich
Sodiumhydroxide		NaOH	BioRad
Agarose	Powder	C12H18O9	BioRad
GelRed			Biotium
50 bp DNA Ladder			Thermo Scientific

Table 7: Overview of reagents used for agarose gel electrophoresis.

EDTA-Buffer (1 mM; pH 8,0):

- 186.12 g EDTA disodium salt was dissolved in approx. 850 ml deionized water
- approx. 20 g sodium hydroxide pellets were dissolved in the solution
- pH 8.0 was adjusted with concentrated sodium hydroxide solution
- the mixture was autoclaved for 15 min at 1.3-1.5 bar at 125 °C

TBE-Buffer (Tris/Borate/EDTA 10x and Tris/Borate/EDTA 0.5x):

- 108 g Tris ultra pure
- 55 g Boric Acid
- 40 ml EDTA-Buffer (pH 8.0) 0,5 M
- mixture was filled up to 100 ml with deionized water
- 50 ml TBE buffer (10x) were resolved in deionized water to a final volume of 1000 ml to receive TBE-Buffer (0.5x)

DNA marker:

1 µl GeneRuler Ultra Low Range DNA ladder (0.5 µg/µl) (Thermo Scientific)
4 µl DNase-free water
1 µl DNA Loading Dye (6x) (Thermo Scientific)

2.4.3 Procedure:

2 % agarose gels with a size of 15x20 cm were used for this study (for smaller sample numbers gels with 7x10 cm were prepared). Agarose (2 % of the mass of the final solution) was dissolved in TBE buffer (0.5 M) by boiling in the microwave. The gel was then cooled to approx. 60 °C in running water. 20 µl GelRed (in case of the smaller gel size 5 µl) were added to the fluid gel and mixed by slewing. Finally the fluid was poured carefully (to avoid air bubble formation) into the clean gel plate. According to sample numbers 2-4 combs were placed in the liquid gel to form wells for sample application. After cooling the agarose set for 20-25 min the combs (and the sidewalls of the plate) could be removed. The electrophoresis chamber was filled with TBE buffer (0.5 M) until the gel was completely submerged.
The DNA marker was prepared as described above and the PCR samples were briefly centrifuged. The loading volume per well was 3 µl or 5 µl according to utilized combs. Depending on the relative sample numbers, big gels with a diameter of 15x20 cm and small gels measuring 7x10 cm were used. After loading of the gel, electrophoresis was carried out by applying a potential across the gels: 50 V for 10 min; 120 V for 50 min (for the small gels 30 min at 100V were sufficient). Visualization of the fluorescing DNA fragments and the bands of the DNA-ladder was performed under UV-light and the banding pattern was photographed with a gel visualizer (GelDoc, BioRad, California).

2.5.1 Detection of somatic mutations by Pyrosequencing®:

Pyrosequencing® via the PyroMark® Q24 MDx System was used as basic technique for detection of point mutations and for mutational analysis across four exons of the *PIK3CA* gene. The sequencing assays covering specific gene sequences within the *PIK3CA* gene were

analyzed under consideration of particular point mutations, stated as most frequent mutations in the *PIK3CA* gene in breast carcinoma according to COSMIC database.
All detected point mutations were confirmed by a second run in which the respective samples were amplified by an independent PCR and sequenced again.

2.5.2 Background:

Pyrosequencing® is a DNA sequencing technique that is based on the "Sequencing by synthesis" principle. A single strand of DNA nucleotides is sequenced as the complementary strand is enzymatically synthesized.
To establish single strand (ss) DNA templates the double stranded PCR products are denaturized chemically. Only biotinylated DNA strands are bound to streptavidin beads whereas the complementary strands are washed away. The biotinylated single stranded template DNA is then hybridized to a sequencing primer. Single stranded template DNA is incubated in an enzyme solution containing DNA polymerase, ATP sulfurylase, luciferase and apyrase as well as the substrates adenosine 5´phosposulfate (APS) and luciferin.
Only one of the four nucleotides is added to the template-enzyme solution at a time. If the nucleotide is complementary to the base of the relative nucleotide in the template strand it is incorporated by the DNA polymerase forming the complementary DNA strand. Incorrect nucleotides are degraded by the apyrase.
The successful incorporation of a nucleotide releases pyrophosphate (PPi). The amount of released pyrophosphate correlates with the number of nucleotides incorporated. The presence of adenosine 5´phophosulfate allows the ATP sulfurylase to convert each pyrophosphate into ATP.
Newly synthesized ATP drives the conversion of luciferin into oxyluciferin which is performed by luciferase causing light emission proportional to the amount of generated ATP. A CCD (charged coupled devices) camera detects the light signals which can be analyzed as peaks in a Pyrogram® employing the PyroMark® Q24 Software. The peak height correlates with the quantity of incorporated nucleotides of (d)ATP, (d)GTP,(d)CTP and (d)TTP allowing the determination of the exact DNA sequence.

2.5.3 Technical facilities

Pyrosequencing® was performed using the PyroMark® Q24 MDx System. With this system preparation of samples, the processing of Pyrosequencing® reactions and analysis of results could be performed.
The PyroMark® Q24 MDx System comprised the following items:

- PyroMark® Q24 MDx Instrument
- PyroMark® Q24 Software for run setup and analysis of results
- PyroMark® Q24 Vacuum Preparation Workstation for preparation of samples
- PyroMark® Q24 Plate to accelerate heat conduction during temperature changes
- PyroMark® Q24 Instrument
- PyroMark® Q24 Troughs
- PyroMark® Q24 Cartridge
- PyroMark® Q24 Gold Reagents

The PyroMark® Q24 Software allowed the specific setup of run files which were transferred to the instrument by USB memory stick. Data from up to 24 samples could be collected simultaneously by 24 CCDs and was shown in form of 24 individual Pyrograms® which could be analyzed with the PyroMark®Q24 Software.

2.5.4 Substrates and Solutions

Table 8 gives an overview of reagents required for the preparation of the Pyrosequencing® reactions.

Reagens	Producer
PyroMark® Binding Buffer	Qiagen (Hilden, Germany)
PyroMark® Denaturation Solution	Qiagen (Hilden, Germany)
PyroMark® Wash Buffer concentrate	Qiagen (Hilden, Germany)
PyroMark® Annealing Buffer	Qiagen (Hilden, Germany)
Strepavidin Sepharose^{TM} High Performance	GE Healthcare (Uppsala, Sweden)
High-purity water ELGA Purelab Ultra(Milli-Q 18.2 MΩ)	ELGA VEOLIA (Paris, France)
Ethanol (70 %)	Chemicals VWR BDH Prolabo, (Radnor, Pennsylvania)

Table 8: Reagents and solutions used for pyrosequencing preparations

Table 9 contains all reagents required for the direct Pyrosequencing® process.

Reagens	Producer
Enzyme Mixture	Qiagen, Hilden
Substrate Mixture	Qiagen, Hilden
dATαS (PyroMark® Q24 Gold Reagent)	Qiagen, Hilden
dGTP (PyroMark® Q24 Gold Reagent)	Qiagen, Hilden
dCTP (PyroMark® Q24 Gold Reagent)	Qiagen, Hilden
dTTP (PyroMark® Q24 Gold Reagent)	Qiagen, Hilden

Table 9: Reagents and solutions required in the pyrosequencing procedure

Enzymes required for the chemical procedure of Pyrosequencing® are DNA polymerase, ATP sulfurylase, luciferase and apyrase which are all comprised in the enzyme mixture (Qiagen, Hilden). Additionally the enzyme mixture contains single-stranded binding proteins (SSB) to inhibit the formation of secondary structures of the DNA template and primers.
The substrate mixture contains adenosine 5´phosphate (APS) and luciferin. Both enzyme and substrate mixture were provided lyophilized by Qiagen and were carefully dissolved in 620 µl high-purity water (Milli-Q 18.2 MΩ).
The nucleotides were already dissolved in a well-balanced buffer system to avoid their degradation. Deoxyadenosine alpha-thio triphosphate (dATPαS) is used instead of the conventional deoxyadenosine triphosphate (dATP) since dATPαS can be efficiently utilized by the DNA polymerase but not by the luciferase.

2.5.5 Pyrosequencing® assays and primers:

For the design of Pyrosequencing® assays and the adequate primers the PyroMark Assay Design Software 2.0 (Version 2.0.1.15) (Qiagen, Hilden, Germany) was used.

Adapted from Nosho et al. (2008) the assays and primers for detection of mutations in exon 20 and 9 of the *PIK3CA* gene were developed (Table 3). In the sequencing assay of exon 9 required utilization of two different primers (9 and 9-3) for complete confirmation of potential mutations.
The primer sequence of exon 9 was slightly modified, whereas the primer sequences of exon 20 and 9-3 were directly adopted from Nosho et al. (2008). Dispensation orders were modified for both exons.
Primers used for the detection of mutations in exon 4 and 7 were newly designed without reference models. (Table 3).

Primer	Exon (of *PIK3CA*)	Nucleotide Sequence 5'→ 3'	Reference
PIK3CA 20	20	GTTGTCCAGCCACCA	[62]
PIK3CA 9	9	TCCATAGAAAATCTTTCTCC	[62]
PIK3CA 9-3	9	TTCTCCTGCTCAGTGATTT	[62]
PIK3CA 7	7	CCCATGCCAATGGAC	
PIK3CA 4	4	GCACTCAGAATAAAAATT	

Table 10: Sequencing-Primers for Pyrosequencing ®

Assay	Primer	Dispensation Order	Hot Spot Mutation
PIK3CA 20	*PIK3CA* 20	TCGACTAGCTGACTATGCACTACGACTGATC GATAGAGATC	c.3140A>G
PIK3CA 9	*PIK3CA* 9	ACTGACGTCGAGTCGACTAGCAGCATGAGAC GTATCATCGCGA	c.1633G>A
PIK3CA 9_1624_Y	*PIK3CA* 9-3	ATGCAGCATGAGACGTATCTGA	c.1624G>A
PIK3CA 7	*PIK3CA* 7	TAGCTGACTCAGTC	c.1258T>C
PIK3CA 4	*PIK3CA* 4	AGCTACGTGCTGATGCTGACAGTCGAGTGTC A	c.1035T>A

Table 11: *PIK3CA* Pyrosequencing® assays with the respective primers and the most commonly occurring mutations in each exon.

The binding sites of the PCR primers and the sequencing primers as well as the target sequence of each exon required for mutational analysis are illustrated in figures 7-10.

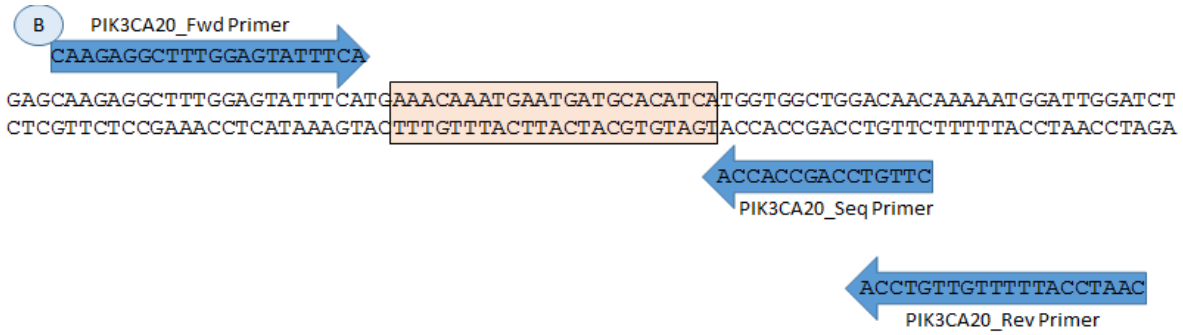

Figure 7: Primer binding sites for Pyrosequencing of *PIK3CA* Exon 20.

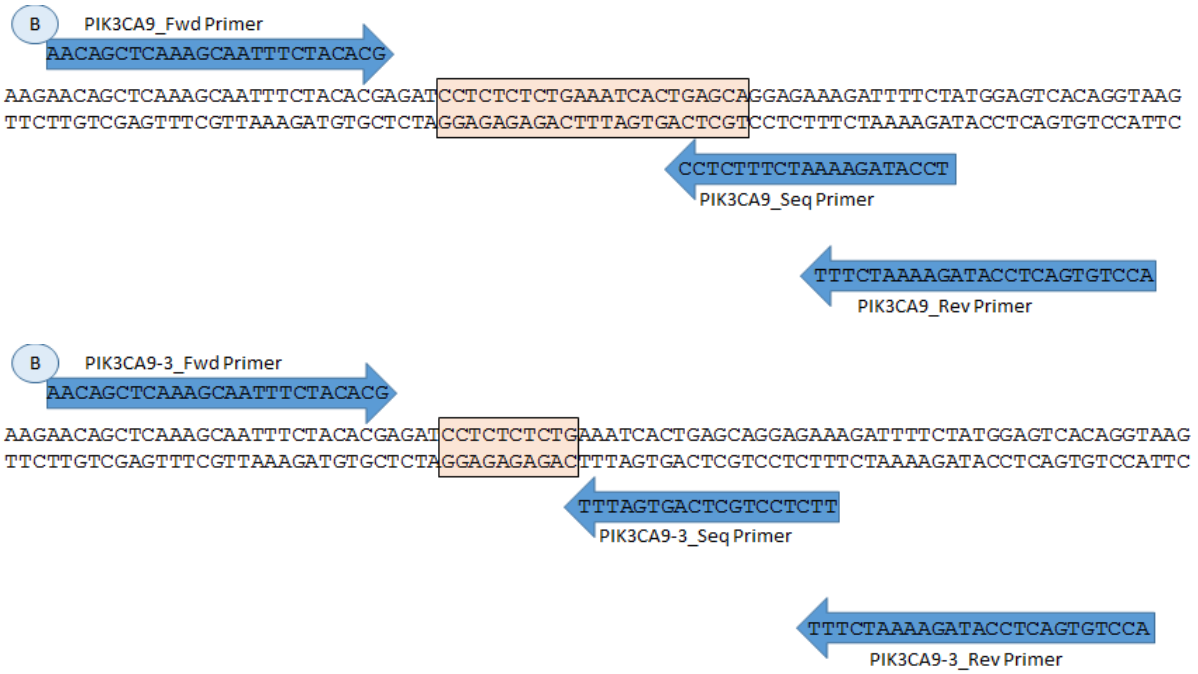

Figure 8: Primer binding sites for Pyrosequencing of *PIK3CA* Exon 9. Pyrosequencing of the PCR products was performed by two different Pyrosequencing primers (Primer *PIK3CA*9 and Primer *PIK3CA*9-3) in order to maximize sensitivity of detection

Figure 9: Primer binding sites for Pyrosequencing of PIK3CA Exon 7. The relevant gene region for sequencing is shown in two sections due to superior overall length.

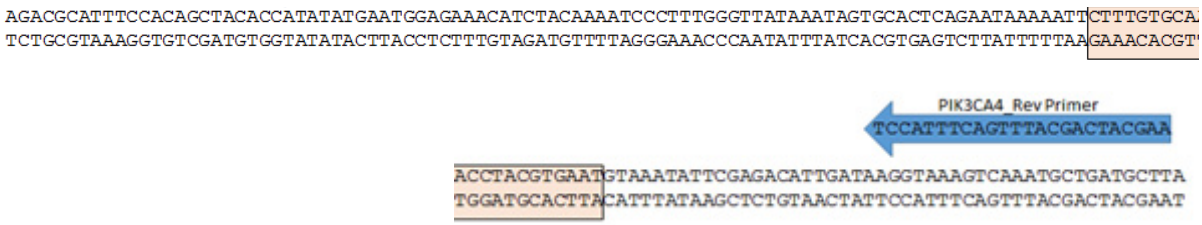

Figure 10: Primer binding sites for Pyrosequencing of *PIK3CA* Exon 4. The relevant gene region for sequencing is shown in two sections due to superior overall length

2.5.6 Sample preparation for immobilization of PCR products on Streptavidin Sepharose High Performance Beads

For the acquisition of single stranded template DNA the biotinylated PCR products were immobilized on streptavidin coated Sepharose™ High Performance beads (GE Healthcare, Uppsala, Sweden). The mastermix for the immobilization reaction was prepared according to table 12.

	Volume per sample	
Reagens	For samples yielding strong bands after electrophoresis	For samples yielding weak bands after electrophoresis
Streptavidin Sepharose HP	2 µl	2 µl
PyroMark® Binding Buffer	40 µl	40 µl
High-purity water	28 µl	18 µl
Subtotal volume	70 µl	60 µl
PCR product	10 µl	20 µl
Total volume	80 µl	80 µl

Table 12: Components composing the solution for DNA immobilization

As 24 Pyrosequencing® reactions could be performed simultaneously the mastermix was prepared for 26 samples to account for pipetting losses. After repeated mixing of the reaction solution the respective final volumes of 70 or 60 µl were pipetted into the wells of a 24-well PCR plate (not skirted) (BRAND GMBH + CO KG, Wertheim, Germany).
The tubes containing the PCR products were thawed and briefly centrifuged.
The visualization of the agarose gel after electrophoresis was now used to evaluate the required amount of template DNA for the sequencing reaction. As strong bands indicate high amounts of PCR product, input of PCR product into the pyrosequencing reaction was determined according to the width and the intensity of bands on the agarose gel. In the case that a sample showed a strong band on the agarose gel after electrophoresis 10 µl of the biotinylated PCR product were added to the reaction mixture. For samples yielding only weak bands on the agarose gel 20 µl of the respective PCR product were used.
The plates were finally agitated on a shaker (1300 rpm) for 10 min to allow binding of the biotinylated PCR product to the streptavidin coated Sepharose^{TM} beads.

In the meantime the sequencing primers mixed with annealing buffer were applied to the wells of a PyroMark Q24 Plate (100) (Qiagen, Hilden, Germany). Thereby the relative primer was diluted with PyroMark® Annealing Buffer (2.5 µl of the relative primer were mixed into 22.5 µl of PyroMark® Annealing Buffer) and pipetted into the according wells of the

PyroMark® Q24 plate (at higher quantities of samples requiring identical primers mastermixes were prepared under consideration of pipetting losses).
In the meantime the sequencing primers were diluted with PyroMark® Annealing Buffer according to table 13 mastermixes were prepared under consideration of pipetting losses. 25 µl of the diluted sequencing primers were applied per well of a PyroMark Q24 Plate (100) (Qiagen, Hilden, Germany).

	Volume per sample
PyroMark® Annealing Buffer	22.5 µl
Sequencing primer	2.5 µl
Total volume	25.0 µl

Table 13: Volumes of pyrosequencing primer and annealing buffer for pyrosequencing preparation

2.5.7 Preparation of the PyroMark® Q24 Vacuum Workstation

The Vacuum Preparation Workstation consists of a Vacuum Preparation Tool and a Worktable. Five PyroMark® Q24 Troughs were assembled into the according basins of the worktable and filled with the respective solutions (approximately 50 ml per trough) as demonstrated in figure 11.
The essential solutions inside the troughs which are essential for the processing of the PCR products are the following:

1. Ethanol (70 %)
2. PyroMark® Denaturation Solution (Qiagen, Hilden, Germany)
3. PyroMark® Wash Buffer (1x) (Qiagen, Hilden, Germany)
4. High-purity water (Milli-Q 18.2 MΩ)
5. High-purity water (Milli-Q 18.2 MΩ)

PyroMark® Wash Buffer was supplied as a 10-fold concentrate and had to be diluted by addition of high-purity water in a 1:10 solution.

The vacuum tool is affiliated with a vacuum pump and allows the absorption and subsequent controlled release of Sepharose™ beads through 24 replaceable filter probes. The plate position on the left on figure 11 is for the 24-well PCR plate (BRAND GMBH + CO KG, Wertheim, Germany) containing the PCR product ligated to the beads. The plate position on the right of figure 11 fits the PyroMark Q24® Plate (Qiagen, Hilden, Germany) which contains the sequencing primer. When not used the Vacuum Preparation Tool is stored in the parking position as shown in figure 11.
Before each preparation procedure the vacuum pump and the vacuum tool was switched on and the filter probes were flushed by the uptake of 50-70 ml of high-purity water. Subsequently the vacuum switch on the tool was turned off and the tool was stored in the parking position until samples were transferred to the workstation. The water trough had to be refilled before each vacuum preparation.

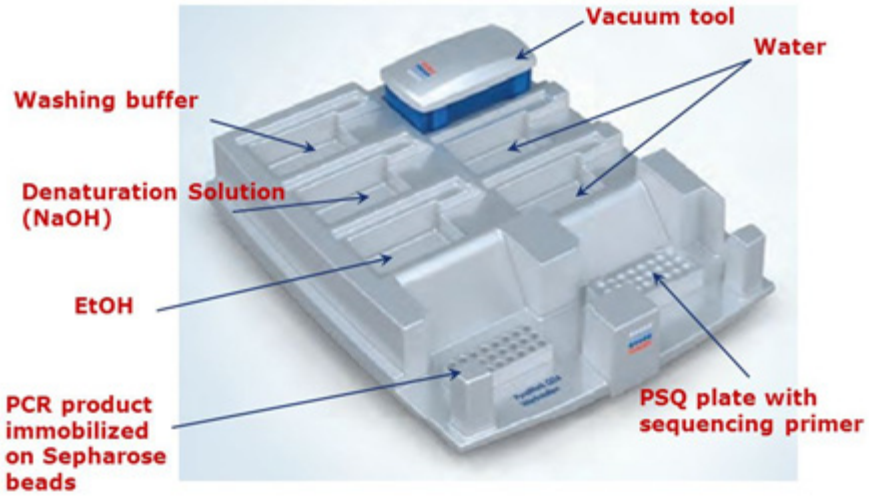

Figure 11: Setup of the PyroMark™Q24 Vacuum Workstation (http://images.slideplayer.us/4/1445547/slides/slide_7.jpg)

2.5.8 Denaturation of PCR products

The PyroMark® Q24 Plate containing the immobilized PCR products (see section 5.4) was taken from the shaker and directly put on the accurate fixture on the Workstation. Vacuum was applied to the vacuum tool and the tool was put into the PCR plate for approximately 15

seconds for the assimilation of up to 24 samples from the separate wells onto the single filter probes. The beads with the bound PCR product were retained on the tips of the filter probes for further treatment while the fluid was aspirated to the waste container.
This step had to be performed very quickly to avoid the sedimentation of the beads in the wells of the PCR plate.
The vacuum tool was then lowered into the trough filled with 70 % ethanol. The filter probes were flushed for approximately 5 seconds and were then held outside the trough for another 5 seconds for draining of residual liquid.
Then the vacuum tool was lowered into the trough containing PyroMark® Denaturation Solution and flushed for 5 seconds. Again 5 seconds of draining of residual liquid followed.
Finally the filter probes were flushed with PyroMark® Wash Buffer (1x) for 10 seconds.
The vacuum tool was vertically raised and overturned beyond 90° to remove all liquid residuals inside and on the surface of the tool.
The vacuum tool was transferred above the PyroMark® Q24 Plate with the before prepared sequencing primers and the vacuum was carefully turned off. After waiting for a few seconds until the remaining vacuum was dispersed, the filter tips were then entirely lowered into the wells of the plate and remaining beads were carefully shaken off.
The filter probes were washed by flushing them with high-purity water after each procedure.

2.5.9 Annealing of sequencing primers

Annealing of sequencing primers to single stranded (denatured) DNA samples was proceeded by heating and subsequent cooling down of the samples.
During the denaturation procedure a plate holder (PyroMark® Q24 Plate Holder, Qiagen, Hilden, Germany) was already heated up in an incubator at 80 °C. The PyroMark® Q24 Plate containing the mixture of respective primers and denatured PCR product bound to beads was placed in the preheated plate holder and immediately put into the incubator at 80 °C for 2 minutes.
Afterwards the PyroMark® Q24 Plate was removed from the plate holder and samples were cooled down for 15 minutes at room temperature, where the annealing of the sequencing primer to the single stranded PCR product took place.
Then the PyroMark® Q24 Plate was placed into the process chamber of the PyroMark® Q24 MDx Instrument.

2.6 Preparation of Pyrosequencing® reagents

The reagents essential for the Pyrosequencing® reaction were all supplied by the PyroMark® Q24 Gold Reagents-set and are listed in table 9. The lyophilized enzyme and substrate mixture had to be reconstituted with 620 µl of high-purity water. The 4 vials containing the nucleotides were shortly centrifuged to avoid bringing crystallizations to the PyroMark® Q24 Cartridge (Qiagen, Hilden, Germany).
Finally the required volume of each reagent was pipetted into the according well of the PyroMark® Q24 Cartridge in a determined order (see PyroMark® Q24 User Manual, 1.02). The filled cartridge was then placed into the dispensing unit of the PyroMark® Q24 MDx Instrument.

2.7 Mutational analysis:

Pyrosequencing results were obtained in form of a Pyrogram and were analyzed by PyroMark® Q24 Application Software 2.0 (Qiagen, Hilden, Germany). Figure 12 shows an example of the spectral output of a pyrosequencing reaction in exon 20 which indicates a mutation from thymine to cytosine (T>C) at position 5. Every detected mutation was confirmed by a second run in order to certainly exclude misleading outputs caused by molecular artefacts.

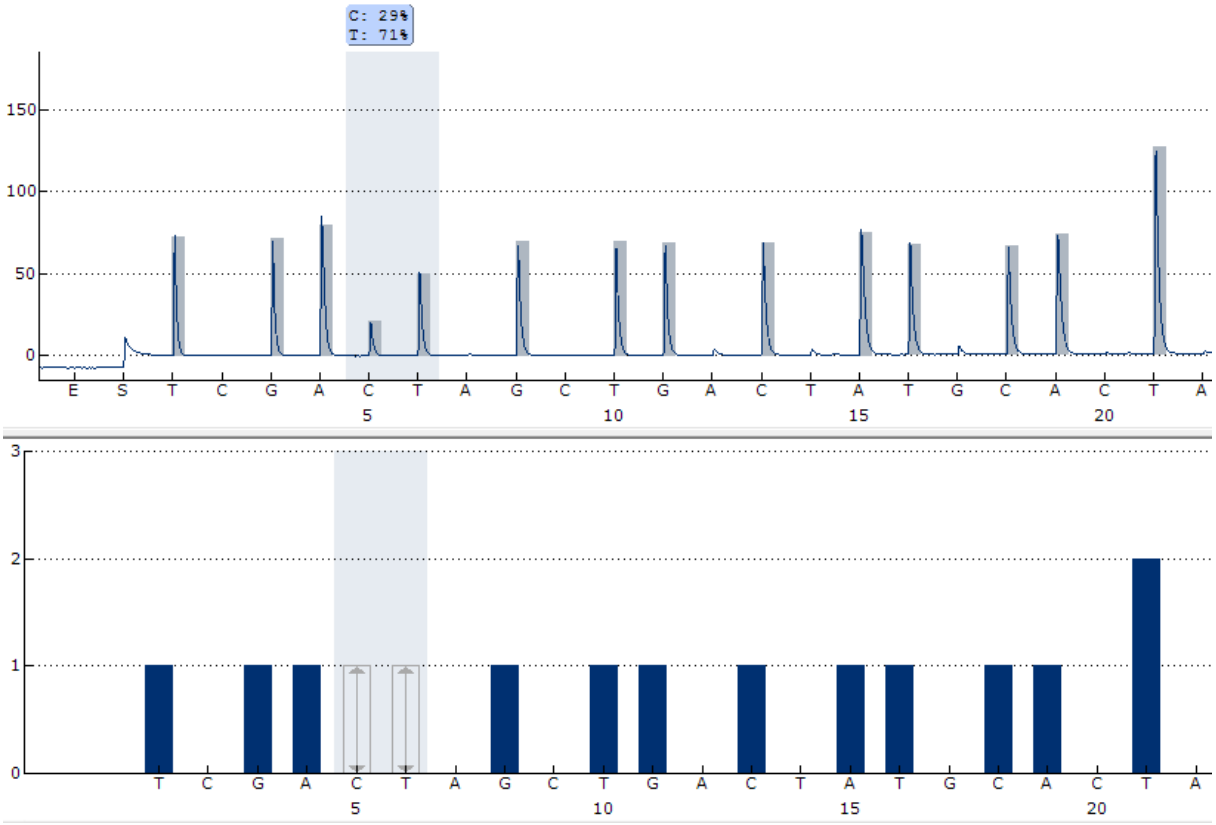

Figure 12: Pyrogram from pyrosequencing reaction. Peaks indicate the relative DNA sequence. Letters below the charts indicate the dispensation order. The bars in the lower scale illustrate the expected base sequence.

2.8.1 Immunohistochemistry for Phopho-S6 Ribosomal Protein and Phospho-mTOR

Immunohistochemical staining for phospho-S6 ribosomal protein (pS6RP) and for phospho-mTOR was performed on sections of 4 µm of the formalin-fixed, paraffin-embedded tissue samples. After manual pretreatment of the samples staining was conducted by Autostainer 360 (LabVision, ThermoScientific, Waltham, Massachusetts) for up to 36 samples automatically. In each run an auxiliary breast carcinoma sample, already proven as positive for phospho-S6RP or phospho-mTOR staining respectively was used as a positive control.

2.8.2 Reagents and Solutions:

10 mM Citrate buffer (used with TBS buffer) (pH 6.0):

- 5.88 g tri-Sodium citrate dihydrate was filled up with deionized water to a final volume of 2000 l
- pH was adjusted to 6.0

10 mM Citrate buffer (used with PBS buffer) (ph 6.0):

- Two stock-solutions were prepared (Stock A and Stock B):

Stock A: 5.25 g Citric acid monohydrate were filled up with deionized water to a final volume of 250 ml
Stock B: 29.4 g tri-Sodium citrate dihydrate were filled up with deionized water to a final volume of 1000 ml

- Stock-solutions were autoclaved at 1.3-1.5 bar at 125 °C for 30 min
- 36 ml of Stock A were mixed to 164 ml of Stock B and the solution was filled up with distilled water to a final volume of 2000 ml
- The pH was adjusted to 6.0

2.8.3 Deparaffinization and pretreatment:

For deparaffinization, tissue sections were first incubated at 65 °C for 10 minutes before they were immersed two times in xylene for one minute. Subsequently sections were hydrated gradually through graded alcohols. Firstly, they were washed in ethanol absolute two times each for one minute, subsequently in 70% ethanol two times each for one minute. To complete rehydration tumor sections were immersed two times for one minute in deionized water.
In the case of phospho-S6RP TBS was used as buffer for treatment in all further steps while PBS buffer was used for phospho-mTOR.
To block the activity of endogenous peroxidases the tissue sections were incubated in solutions of 0.3% H_2O_2 in TBS/PBS for 10 minutes at room temperature.

For antigen retrieval slides were boiled for 10 min in 10 mM citrate buffer and a pressure of approximately 1.5 bar was applied for 2.5 minutes during the boiling process.
After cooling down at room temperature for 15 minutes the slides were immersed in TBS/PBS containing 0.1% Tween 20 for 3 minutes.

2.8.4 Automated processing with Autostainer 360:

All steps performed by the autostainer took place at room temperature and were controlled under supervision.
Blocking was conducted by treatment of the sections with Ultra V Block (UltraVision LP Large Volume Detection System HRP Polymer, Lab Vision, Waltham, Massachusetts, catalogue number TL-125-HL) for 5 minutes.
Prior to antibody application the blocking solution was removed with air.
The primary antibody against phospho-S6 Ribosomal Protein (Ser240/244) (D68F8) XP® (Rabbit Monoclonal Antibody, Cell Signaling, Danvers Massachusetts, catalogue #5364) was used in a 1:1000 dilution with SignalStain® Antibody Diluent (Cell Signaling, Danvers Massachusetts, catalogue #8112). Incubation with the primary antibody was conducted for 30 minutes.
In the case of phospho-mTOR the antibody phospho-mTOR (Ser2448) (49F9) (Rabbit Monoclonal Antibody, Cell Signaling, Danvers Massachusetts , catalogue #2976) was diluted 1:100 in PBS + 0.1% Tween 20 containing Goat Serum (normal) (Dako, Glostrup, Denmark catalogue X0907) in a 1:100 dilution. The antibody was incubated overnight at 4 °C.
For the detection of antibody binding the UltraVision LP Large Volume Detection System HRP Polymer (Lab Vision Corporation, Fremont, California, catalogue # TL-125-HL) was used.
Firstly, the sections were washed two times with TBS/PBS containing 0.1% Tween 20. Incubation with Primary Antibody Enhancer (UltraVision LP) for 10 minutes followed. Again the sections were washed two times with TBS/PBS containing 0.1% Tween 20. Incubation with HRP Polymer (UltraVision LP) took place for 15 minutes. After washing two times with TBS or PBS containing 0.1% Tween 20, a solution of Liquid DAB+ Chromogen and Substrate Buffer (Dako, Dako, Glostrup, catalogue K3468, 20 µl of DAB+ Chromogen were added per milliliter of DAB+ Substrate Buffer) was applied for 10 minutes for phospho-S6RP staining and 5 minutes for phospho-mTOR staining.

At the end of this incubation the sections were rinsed with deionized water and were ready for counterstaining.

2.8.5 Counterstaining with Gill´s Hematoxylin no. 3:

The counterstaining was performed manually for 20 seconds in Gill´s Hematoxylin no. 3 and yielded a blue staining of the cell nuclei. Afterwards, the sections were rinsed in tap water and deionized water two times each.
Subsequently the tissue sections were dehydrated by immersion in graded alcohols (70%, 80%, 96%, 100%) for 10-15 seconds each. Finally incubation in Ethyl-n-*butyl* ether (EBE) concluded the procedure and the slides were carefully mounted with Entellan (Merck Millipore, Darmstadt, Germany catalogue# 1.07961.0100).

2.8.6 Statistical analysis:

In our study distant recurrence-free survival (DRFS) was chosen as primary endpoint. DRFS is defined as the time frame from randomization of patients to the first occurrence of invasive cancer recurrence at a distant site [63].

The comparison of baseline characteristics from patients of ABCSG6a with the study cohort was performed by using chi-square tests. Correlation with age was tested using a Mann-Whitney-Test. Chi-square test was utilized to test the potential correlations of baseline characteristics with the parameters determined in this study (phospho-mTOR, phospho-S6RP and *PIK3CA*-status). Values for phospho-mTOR and phospho-S6RP were dichotomized to low and high, with a score $\leq$20 defining low and >20 defining high. The parameter of *PIK3CA*-status was defined as the presence (mutations) or absence (wildtype) of any of the detected mutations.

Survival rates were estimated with the use of the Kaplan-Meier method. Survival curves were compared by applying a log-rank-test. Univariate and multiple Cox-Regression models were used to study the prognostic and predictive value of the collected parameters. Multiple regression models included all collected tumor parameters; age, tumor size, lymph node status, tumor grade, ER expression, PgR expression, and adjuvant endocrine treatment. Only

P-values equal or less than 5% were considered statistically significant. Furthermore the P-values reported below are solely results of two-sided tests. Statistical analyses were performed employing SPSS software, version 15.0 (SPSS Inc.; IBM Armonk, New York). Kaplan Meier curves were designed with the software program STATISTICA, version 8.0 (StatSoft, Tulsa, Oklahoma).

Results

3.1 Sample collection & patient characteristics:

Formalin-fixed, paraffin-embedded tumor blocks were available from 546 out of 856 (64%) patients from ABCSG 6a. In total, 21 centers contributed tumor specimens. All tumor samples were obtained at the time of surgery before adjuvant treatment. Tumor blocks were stored at room temperature and were identifiable only by an identification number assigned to each block at diagnosis. Approval was obtained from the local Institutional Review Board. From each tumor block sections were cut at 4 µm. One section was stained by hematoxylin and eosin to confirm the presence of invasive carcinoma histologically and further sections were used for subsequent DNA isolation and immunohistochemistry. After histological evaluation, 19 cases were excluded due to insufficient amounts of invasive carcinoma. Thus, 527 tumor blocks were available for further analyses.

Next, we analyzed the distribution of the major clinical parameters of patients with tumor blocks compared to the total study population. As shown in table 14, no significant differences in baseline variables between patients from our study subset and the total ABCSG 6a patient population were observed. Therefore, our study population is representative for ABCSG trial 6a.

Characteristics	ABCSG 6a n=856	Study population n=527
Age, years		
Median	68.1	67.9
Range	51.8-85.5	51.8-84.5
Tumor size		
T1	537 (62.7%)	329 (62.4%)
T2	303 (35.4%)	188 (35.7%)
T3	16 (1.9%)	10 (1.9%)
Nodal status		
Negative	578 (67.5%)	347 (65.8%)
1 to 3 positive nodes	216 (25.2%)	137 (26.0%)
4-10 ositive nodes	49 (5.7%)	37 (7.0%)
>10 positive nodes	13 (1.5%)	6 (1.1%)
Tumor grade		
G1	146 (17.1%)	99 (18.8%)
G2	476 (55.6%)	304 (57.7%)
G3	171 (20.0%)	90 (17.1%)
GX	63 (7.4%)	34 (6.5%)
Estrogen receptor†		
Negative	19 (2.2%)	7 (1.3%)
Low	167 (19.5%)	109 (20.7%)
Medium	305 (35.6%)	193 (36.6%)
High	337 (39.4%)	211 (40.0%)
Unknown	28 (3.3%)	7 (1.3%)
Progesterone receptor†		
Negative	140 (16.4%)	85 (16.1%)
Low	175 (20.4%)	116 (22.0%)
Medium	234 (27.3%)	143 (27.1%)
High	277 (32.4%)	174 (33.0%)
Unknown	30 (3.5%)	9 (1.7%)
Pretreatment*		
Tamoxifen	451 (52.7%)	292 (55.4%)
Tamoxifen plus aminoglutethimide	405 (47.3%)	235 (44.6%)

Table 14: Patient characteristics.

*Adjuvant treatment received in ABCSG Trial 6

3.2.1 *PIK3CA* mutation analysis:

In 505 out of 527 (96%) patients, complete data on the *PIK3CA* mutation status from all 4 investigated exons (exon 4, 7, 9, and 20) were available and statistical analyses were performed in these cases. *PIK3CA* point mutations were detected in 214 out of 505 (42.4%) tumor samples. A total of 16 distinct somatic mutations were identified. Among these, six mutations were previously unknown and not registered in the Cosmic Database (table 15). Of these new mutations p.S541F and p.K417N were only found in context with other mutations within the same sample.

New Mutations		
Exon	Mutation	Frequency
4	p.C340Y	4
4	p.Y343F	1
7	p.E418D	2
7	p.K417N	1
7	p.H419Y	1
9	p.S541F	1

Table 15: New mutations in the *PIK3CA* gene

Overall 20 complex mutations were identified as well (table 16). Within this group eight pairs of point mutations solely occurred in exon 20. Furthermore three pairs were detected in exon 9 and one pair in exon 7. The remaining eight complex mutations were spread over different exons. Three complex mutations were localized to exon 20 and exon 4 and another three to exon 20 and exon 9. In one sample, triple-mutations in exon 20, 9 and 4 were detected and in another tumor sample exon 20 harbored two mutations simultaneously with one mutation in exon 4.

Mutations	**Number**	**%**
Single new mutations	4	0.8
Complex mutations	20	4
p.C420R	3	0.6
p.E542K	20	4
p.E545A	4	0.8
p.E545K	46	9.1
p.E545Q	1	0.2
p.H1047L	11	2.2
p.H1047R	91	18
p.M1043I	1	0.2
p.N1044S	1	0.2
p.N345K	9	1.8
p.Q546K	3	0.6
Total mutations	**214**	**42.4**

Table 16: Summary of *PIK3CA* mutations

Exon 20 (kinase domain) and exon 9 (helical domain) were the most frequent mutations and account together for more than 37% of mutated samples whereas in the C2 domain only one type of mutational substitution could be identified in both, exon 4 and 7. The three hotspot mutations p.H1047R (42%), p.E545K (21%) and p.E542K (9%) together account for over 73% of detected *PIK3CA* mutations.

Exon	Frequency	%
Exon 9	77	15.2
Exon 20	112	22.2
Subtotal	**189**	**37.4**
Exon 4	11	2.2
Exon 7	6	1.2
Subtotal	**17**	**3.4**
Complex	8	1.6
Total	**214**	**42.4**

Table 17: Distribution of mutations over the 4 distinct exons and their absolute and relative frequencies. Complex designates complex mutations which occur in different exons of the same sample.

3.2.2 Correlation of *PIK3CA* Mutations with Clinicopathologic Risk Factors:

Next, we analyzed the correlation of *PIK3CA* mutations with clinicopathologic risk factors. The associations of *PIK3CA* mutational status with clinical parameters are shown in table 18. However, no significant correlation between *PIK3CA* mutations and age, tumor size, nodal status, tumor grade, ER expression, PgR expression and adjuvant treatment was observed (Table 18).

Characteristic	Total n=505	*PIK3CA* wildtype n=291	*PIK3CA* mutant n=214	P
Age, years				0.27
Median	68.2	68.6	67.6	
Range	51.8-84.5	53.2-83.5	51.8-84.5	
Tumor size				0.93
T1	314 (62.2%)	183 (62.9%)	131 (61.2%)	
T2	182 (36.0%)	103 (35.4%)	79 (36.9%)	
T3	9 (1.8%)	5 (1.7%)	4 (1.9%)	
Nodal status				0.1
Negative	334 (66.1%)	202 (69.4%)	132 (61.7%)	
1 to 3 positive nodes	130 (25.7%)	68 (23.4%)	62 (29.0%)	
4-10 positive nodes	35 (6.9%)	16 (5.5%)	19 (8.9%)	
>10 positive nodes	6 (1.2%)	5 (1.7%)	1 (0.5%)	
Tumor grade				0.2
G1	93 (18.4%)	47 (16.2%)	46 (21.5%)	
G2	292 (57.8%)	168 (57.7%)	124 (57.9%)	
G3	86 (17.0%)	57 (19.6%)	29 (13.6%)	
GX	34 (6.7%)	19 (6.5%)	15 (7.0%)	
Estrogen receptor				0.76
Negative	6 (1.2%)	3 (1.0%)	3 (1.4%)	
Low	104 (20.9%)	56 (19.4%)	48 (23.0%)	
Medium	183 (36.7%)	109 (37.7%)	74 (35.4%)	
High	205 (41.2%)	121 (41.9%)	84 (40.2%)	
Unknown				
Progesterone receptor				0.19
Negative	82 (16.5%)	52 (18.1%)	30 (14.4%)	
Low	110 (22.2%)	67 (23.3%)	43 (20.6%)	
Medium	139 (28.0%)	70 (24.4%)	69 (33.0%)	
High	165 (33.3%)	98 (34.1%)	67 (32.1%)	
Unknown				
Pretreatment				0.50
Tamoxifen	265 (52.5%)	149 (51.2%)	116 (54.2%)	
Tamoxifen plus aminoglutethimide	240 (47.5%)	142 (48.8%)	98 (45.8%)	
Treatment arm				0.43
No further treatment	277 (54.9%)	164 (56.4%)	113 (52.8%)	
3 years anastrozole	228 (45.1%)	127 (55.7%)	101 (47.2%)	

Table 18: Characteristics of patients according to *PIK3CA* mutational status.

3.2.3 Prognostic analysis of *PIK3CA* mutational status:

A total of 39 of 527 patients (7.4%) whose tumor tissues were analyzed in this study developed distant metastases and 74 of 527 patients (14%) died. The median follow-up of the study population was 6.6 years and the primary endpoint of the study was distant recurrence-free survival (DRFS).

In univariate survival analyses, tumor size (hazard ratio [HR] for distant recurrence 1.83; 95% CI 1.07 to 3.14; P=0.03), lymph node status (HR for distant recurrence 3.24; 95% CI 2.36 to 4.47; P<0.001), and PgR expression (HR for distant recurrence 0.74; 95% CI 0.55 to 0.98; P=0.03) were significantly associated with DRFS (Table 19). Age, grading, ER expression, and treatment arm were not associated with DRFS. There were also no DRFS differences between patients harboring *PIK3CA* mutations and *PIK3CA* wildtype patients (HR for distant recurrence 1.22; 95% CI 0.65 to 2.32; P=0.53) (Table 19, Figure 13).

Variable	Hazard ratio for distant recurrence	95% CI*	P
Age	0.71	0.37-1.36	0.30
Tumor size	1.83	1.07-3.14	0.03
Nodal status	3.24	2.36-4.47	<0.001
Tumor grade	1.03	0.69-1.55	0.88
ER	0.73	0.50-1.06	0.10
PgR	0.74	0.55-0.98	0.03
Treatment arm	0.71	0.37-1.36	0.30
PIK3CA mutations	1.22	0.65-2.32	0.53

Table 19: Univariate Cox proportional hazards models.
*95% CI = 95% confidence interval.
Variables were coded as described in Table 14.

If patients were split into the two categories wildtype and kinase domain mutations (exon 20) plus helical domain mutations (exon 9), also no differences in DRFS were observed (HR for distant recurrence 1.04; 95% CI 0.52 to 2.10; P=0.90).

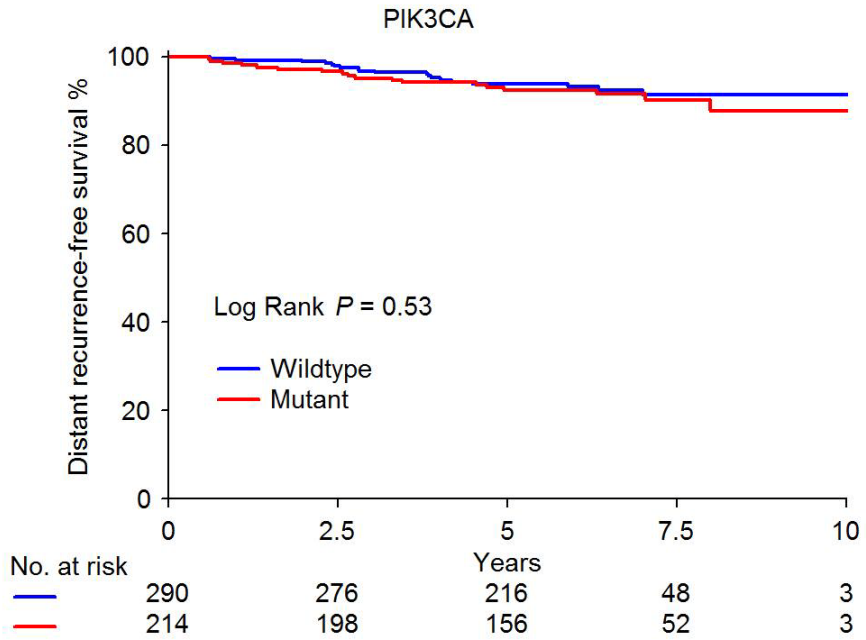

Figure 13: Kaplan-Meier plot of the probability of DRFS according to *PIK3CA* mutation status.

In order to evaluate a potential independent prognostic value of *PIK3CA* mutations, a multivariate Cox model was performed. In this model, *PIK3CA* mutations were studied simultaneously with age, tumor size, nodal status, tumor grade, ER expression, PgR expression, and treatment arm. In these multivariate analyses, only lymph node status and PgR expression were significantly associated with DRFS (adjusted HR for distant recurrence 3.13, 95% CI 2.18-4.50, P<0.001 and 0.72, 95% CI 0.53-0.97, P=0.03, respectively) (Table 20). *PIK3CA* mutations were not associated with DRFS of the patients (adjusted HR for distant recurrence 1.27, 95% CI 0.65-2.47, P=0.48) (Table 20). Thus, only lymph node status and PgR expression were independent prognostic factors. *PIK3CA* mutations had no prognostic value.

Variable	Hazard ratio for distant recurrence	95% CI*	P
Age	0.98	0.94-1.02	0.34
Tumor size	1.25	0.65-2.42	0.51
Nodal status	3.13	2.18-4.50	<0.001
Tumor grade	0.74	0.46-1.22	0.24
ER	0.86	0.57-1.29	0.45
PgR	0.72	0.53-0.97	0.03
Treatment arm	0.83	0.42-1.62	0.58
PIK3CA mutations	1.27	0.65-2.47	0.48

Table 20: Multivariate Cox proportional hazards model.

*95% CI = 95% confidence interval.

Variables were coded as described in Table 14.

3.2.4 Predictive analysis of *PIK3CA* mutational status

The interaction of *PIK3CA* mutations and extended adjuvant treatment was evaluated in a Cox model that included age, tumor size, nodal status, tumor grade, ER expression, PgR expression, treatment arm, *PIK3CA* mutations, and an interaction term, the product of *PIK3CA* mutations and treatment arm. In this model, the interaction term was not significant (P=0.78) and, therefore, *PIK3CA* mutations have no predictive value in our study population (Table 21).

Variable	Hazard ratio for distant recurrence	95% CI*	P
Age	0.98	0.93-1.02	0.33
Tumor size	1.25	0.65-2.41	0.51
Nodal status	3.15	2.19-4.55	<0.001
Tumor grade	0.75	0.46-1.22	0.25
ER	0.86	0.57-1.30	0.47
PgR	0.72	0.53-0.97	0.03
Treatment arm	0.91	0.36-2.33	0.84
PIK3CA mutations	1.65	0.23-11.91	0.62
PIK3CA mutations x treatment arm	0.83	0.22-3.18	0.78

Table 21: Interaction analysis.

*95% CI = 95% confidence interval.

Variables were coded as described in Table 14.

3.3.1 Phospho-mTOR immunohistochemistry

Phospho-mTOR staining was evaluable in 518 of 527 (98%) tumor samples and all further statistical analyses were performed on this patient population. We assessed tumor phospho-mTOR expression using standard immunohistochemistry as described in the methods section. Immunostaining of phospho-mTOR was predominantly cytoplasmatic. Figure 14 shows representative examples of phospho-mTOR immunostaining. Comparisons of phospho-mTOR expression with clinical parameters including survival of the patients were performed with phospho-mTOR expression as a dichotomized variable classified as high or low. Of the 518 tumors, 318 (61%) showed low phospho-mTOR expression and 200 (39%) high phospho-mTOR expression.

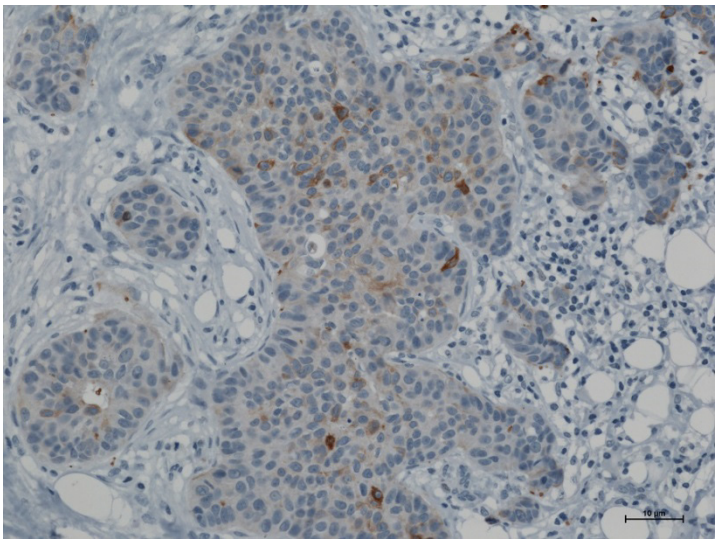

(a)

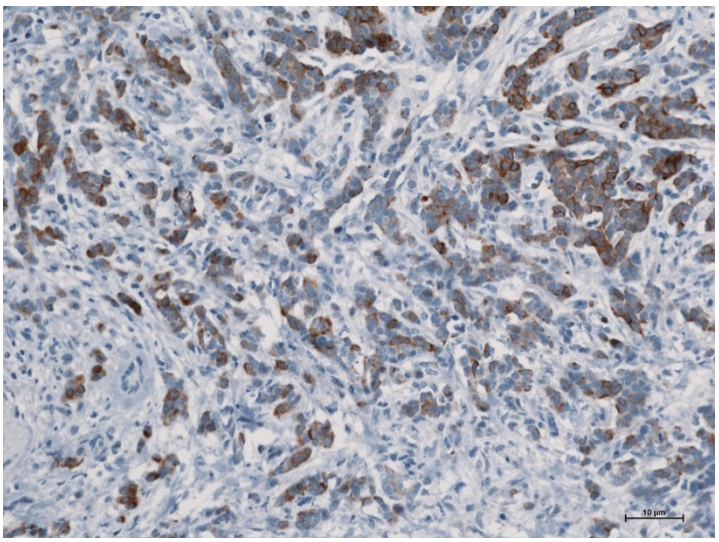

(b)

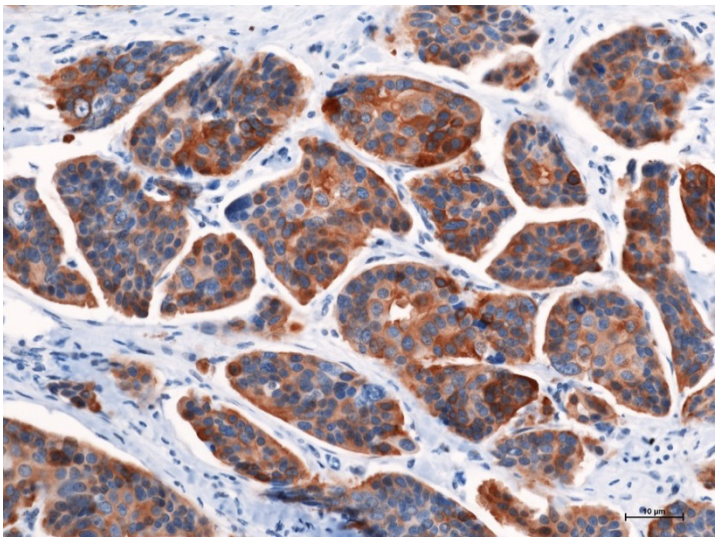

(c)

Figure 14: Representative examples of phospho-mTOR (a-c) immunohistochemical staining in samples of invasive breast carcinoma. Original magnification, x200

3.3.2 Correlation of phospho-mTOR with Clinicopathologic Risk Factors:

We analyzed the correlation between phospho-mTOR status and clinicopathologic parameters of the patients. The associations of phospho-mTOR expression with clinical parameters are shown in table 22. However, no significant correlation between phospho-mTOR expression and age, tumor size, nodal status, tumor grade, ER expression, PgR expression and treatment arm was observed (Table 22). We also studied the relationship between *PIK3CA* mutations and phospho-mTOR expression. High phospho-mTOR expression was more frequently observed in patients with *PIK3CA* mutations compared to patients with *PIK3CA* wildtype status (44% versus 36%; P=0.08). However, this difference did not reach the level of statistical significance.

Characteristic	Total n=518	p-mTOR low n=318	p-mTOR high n=200	P
Age, years				0.54
Median	68.0	68.0	67.9	
Range	51.8-84.5	51.8-84.5	54.9-83.6	
Tumor size				0.23
T1	321 (62.0%)	206 (64.8%)	115 (57.5%)	
T2	187 (36.1%)	107 (33.6%)	80 (40.0%)	
T3	10 (1.9%)	5 (1.6%)	5 (2.5%)	
Nodal status				0.55
Negative	340 (65.6%)	214 (67.3%)	126 (63%)	
1 to 3 positive nodes	135 (26.1%)	81 (25.5%)	54 (27%)	
4-10 positive nodes	37 (7.1%)	19 (6.0%)	18 (9.0%)	
>10 positive nodes	6 (1.2%)	4 (1.3%)	2 (1.0%)	
Tumor grade				0.27
G1	97 (18.7%)	59 (18.6%)	38 (19.0%)	
G2	298 (57.5%)	188 (59.1%)	110 (55.0%)	
G3	90 (17.4%)	56 (17.6%)	34 (17.0%)	
GX	33 (6.4%)	15 (4.7%)	18 (9.0%)	
Estrogen receptor†				0.7
Negative	7 (1.4%)	5 (1.6%)	2 (1.0%)	
Low	107 (20.9%)	62 (19.8%)	45 (22.7%)	
Medium	191 (37.4%)	122 (39.0%)	69 (34.8%)	
High	206 (40.3%)	124 (39.6%)	82 (41.4%)	
Unknown				
Progesterone receptor†				0.18
Negative	82 (16.1%)	56 (18.0%)	26 (13.1%)	
Low	116 (22.8%)	75 (24.1%)	41 (20.7%)	
Medium	139 (27.3%)	76 (24.4%)	63 (31.8%)	
High	172 (33.8%)	104 (33.4%)	68 (34.3%)	
Unknown				
Treatment arm				0.46
No further treatment	290 (56.0%)	174 (54.7%)	116 (58%)	
3 years anastrozole	228 (44.0%)	144 (45.3%)	84 (42.0%)	

Table 22: Characteristics of patients according to phospho-mTOR expression..

3.3.3 Prognostic analysis of phospho-mTOR status:

In univariate survival analyses, DRFS was not significantly different between patients with low or high phospho-mTOR expression in their tumors (HR for distant recurrence 1.57; 95% CI 0.84 to 2.93; P=0.16).

The independent effect of phospho-mTOR expression on DFRS was assessed by a Cox proportional hazards regression model adjusted for age, tumor size, lymph node status, tumor grade, ER expression, PgR expression, and treatment arm (Table 23). In these analyses, phospho-mTOR expression was not significantly associated with DFRS (adjusted HR for distant recurrence 1.50; 95% CI 0.79 to 2.83; P=0.22) (Table 23). Thus, phospho-mTOR has no prognostic value.

Variable	Hazard ratio for distant recurrence	95% CI*	P
Age	0.95	0.93-1.02	0.27
Tumor size	1.27	0.66-2.44	0.48
Nodal status	3.27	2.28-4.67	<0.001
Tumor grade	0.66	0.4-1.07	0.09
ER	0.84	0.56-1.26	0.41
PgR	0.72	0.53-0.97	0.03
Treatment arm	0.84	0.43-1.64	0.61
Phospho-mTOR	1.50	0.79-2.83	0.22

Table 23: Multivariate Cox proportional hazards model.
*95% CI = 95% confidence interval.
Variables were coded as described in Table 14.

3.3.4 Predictive analysis of phospho-mTOR status:

Again a Cox-regression model adjusted for patient's age, tumor size, nodal status, tumor grade, ER expression, PgR expression, treatment arm, and an interaction term, the product of phospho-mTOR expression and treatment arm was used to determine the predictive value of phospho-mTOR expression. Interestingly, a significant interaction between phospho-mTOR expression and treatment arm was detected (P=0.03) (Table 24). For patients classified as phospho-mTOR high, a significant treatment effect was observed, with the hazard of a DRFS event being greater for the observation group compared to patients treated with extended endocrine therapy (P=0.02) (Figure 15). In contrast, no statistically significant effect of extended endocrine treatment was detected for phospho-mTOR low (P=0.34) (Figure 16), indicating that phospho-mTOR low patients derived little or no benefit from extended endocrine treatment. Our findings suggest that postmenopausal women with high phospho-mTOR expression appear to benefit from extension of endocrine therapy after 5 years of treatment with tamoxifen, whereas patients with low phospho-mTOR expression do not.

Variable	**Hazard ratio for distant recurrence**	**95% CI***	**P**
Age	0.97	0.93-1.02	0.2
Tumor size	1.34	0.7-2.57	0.38
Nodal status	3.17	2.21-4.56	<0.001
Tumor grade	0.69	0.43-1.13	0.14
ER	0.82	0.55-1.24	0.35
PgR	0.75	0.56-1.02	0.06
Treatment arm	1.68	0.69-4.09	0.25
Phospho-mTOR	14.95	1.82-122.67	0.01
Phospho-mTOR x treatment arm	0.18	0.04-0.83	0.03

Table 24: Interaction analysis.

*95% CI = 95% confidence interval.

Variables were coded as described in Table 14.

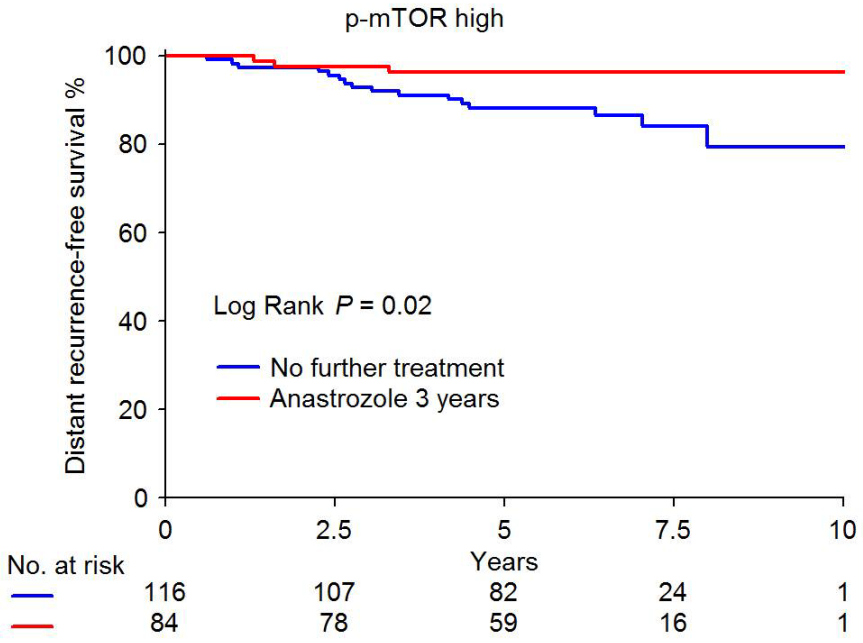

Figure 15: Kaplan-Meier plot of DRFS according to treatment arm in patients with high phospho-mTOR expression.

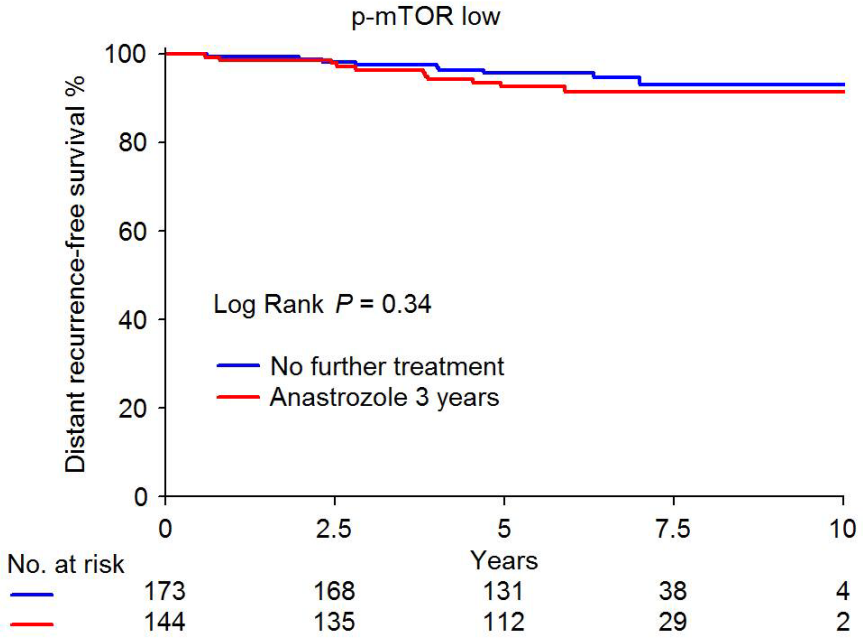

Figure 16: Kaplan-Meier plot of DRFS according to treatment arm in patients with low phospho-mTOR expression.

3.4.1 phospho-S6RP immunohistochemistry

Phospho-S6RP staining was evaluable in 509 of 527 (97%) tumor samples and all further statistical analyses were performed on these patients. We assessed tumor phospho-S6RP expression using standard immunohistochemistry as described in the methods section. Immunostaining of phospho-S6RP was predominantly cytoplasmatic. Figure 17 shows representative examples of phospho-S6RP immunostaining. Comparisons of phospho-S6RP expression with clinical parameters including survival of the patients were performed with phospho-S6RP expression as a dichotomized variable classified as high or low. Of the 509 tumors, 396 (78%) showed low phospho-S6RP expression and 113 (22%) high phospho-S6RP expression.

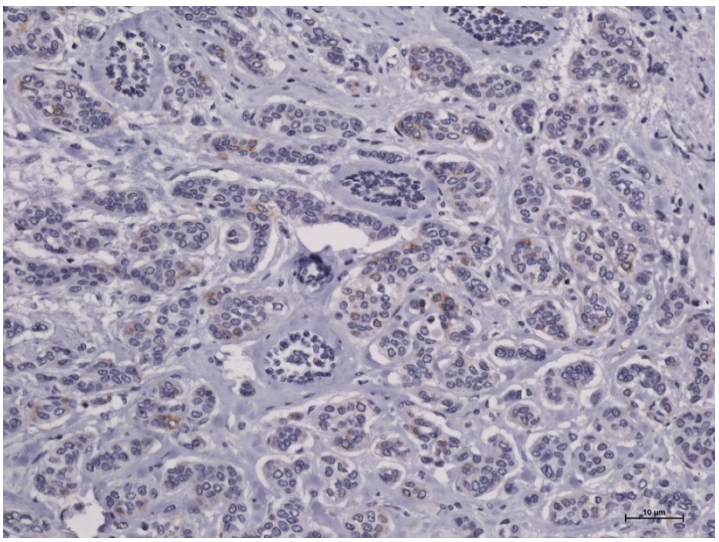

(a)

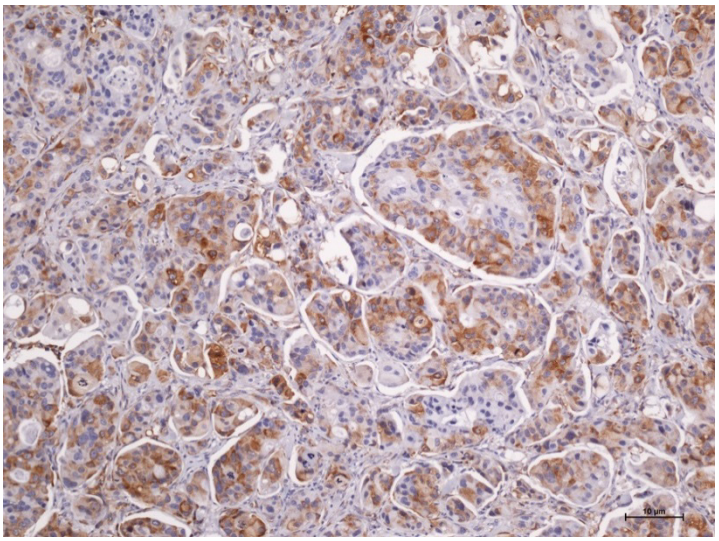

(b)

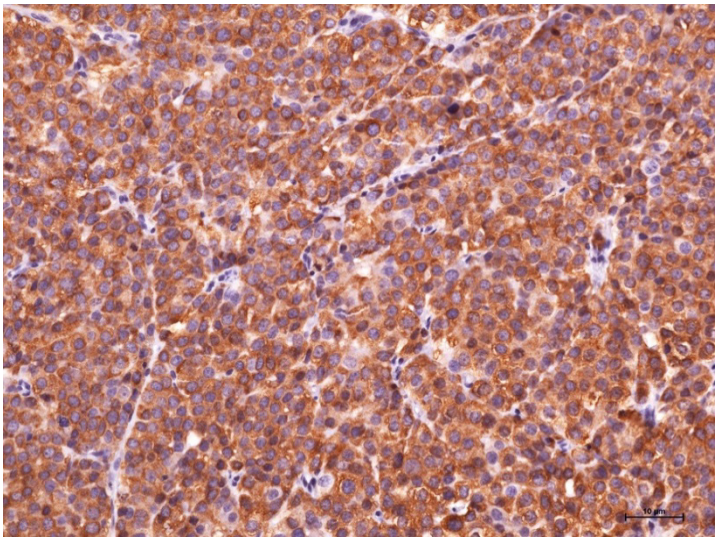

(c)

Figure 17: Representative example of phospho-S6RP (a-c) immunohistochemical staining in samples of invasive breast carcinoma. Original magnification, x200

3.4.2 Correlation of phospho-S6RP with Clinicopathologic Risk Factors:

The association of phospho-S6RP expression with clinical parameters is shown in table 25. However, no significant correlation between phospho-S6RP expression and age, tumor size, nodal status, tumor grade, ER expression, PgR expression and extended adjuvant treatment was observed (Table 25). In addition, no correlation between phospho-S6RP expression and phospho-mTOR expression as well as *PIK3CA* mutations was observed (P=0.37 and P=0.65, respectively).

Characteristic	Total n=509	p-S6RP low n=396	p-S6RP high n=113	P
Age, years				0.48
Median	67.9	68.2	66.9	
Range	51.8-84.5	51.8-84.5	54.2-83.6	
Tumor size				0.41
T1	315 (61.9%)	239 (60.4%)	76 (67.3%)	
T2	184 (36.1%)	149 (37.6%)	35 (31.0%)	
T3	10 (2.0%)	8 (2.0%)	2 (1.8%)	
Nodal status				0.63
Negative	336 (66.0%)	260 (65.7%)	76 (67.3%)	
1 to 3 positive nodes	130 (25.5%)	101 (25.5%)	29 (25.7%)	
4-10 positive nodes	37 (7.3%)	29 (7.3%)	8 (7.1%)	
>10 positive nodes	6 (1.2%)	6 (1.5%)	0 (0.0%)	
Tumor grade				0.07
G1	94 (18.5%)	75 (18.9%)	19 (16.8%)	
G2	294 (57.8%)	236 (59.6%)	58 (51.3%)	
G3	88 (17.3%)	59 (14.9%)	29 (25.7%)	
GX	33 (6.5%)	26 (6.6%)	7 (6.2%)	
Estrogen receptor†				0.09
Negative	6 (1.2%)	3 (0.8%)	3 (2.7%)	
Low	105 (20.9%)	77 (19.8%)	28 (24.8%)	
Medium	185 (36.9%)	140 (36.0%)	45 (39.8%)	
High	206 (41.0%)	169 (43.4%)	37 (32.7%)	
Unknown				
Progesterone receptor†				0.07
Negative	83 (16.6%)	63 (16.3%)	20 (17.7%)	
Low	112 (22.4%)	78 (20.2%)	34 (30.1%)	
Medium	139 (27.8%)	108 (27.9%)	31 (27.4%)	
High	166 (33.2%)	138 (35.7%)	28 (24.8%)	
Unknown				
Treatment arm				0.42
No further treatment	281 (55.2%)	220 (55.6%)	61 (54%)	
3 years anastrozole	228 (44.8%)	176 (44.4%)	52 (46%)	

Table 25: Characteristics of patients according to phospho-S6RP expression.

pS6RP=phospho-S6RP

3.4.3 Prognostic analysis of phospho-S6RP:

In univariate survival analyses, DRFS was not significantly different between patients with low phospho-S6RP expression in their tumors and patients high phospho-S6RP expression (HR for distant recurrence 0.61; 95% CI 0.26 to 1.46; P=0.27).

The independent effect of phospho-S6RP expression on DFRS was assessed by a Cox proportional hazards regression model adjusted for age, tumor size, lymph node status, tumor grade, ER expression, PgR expression, and treatment arm (Table 26). In these analyses, phospho-S6RP expression was not significantly associated with DFRS (adjusted HR for distant recurrence 0.70; 95% CI 0.29 to 1.70; P = 0.42) (Table 26). Thus, phospho-S6RP expression has no prognostic value.

Variable	**Hazard ratio for distant recurrence**	**95% CI***	**P**
Age	0.98	0.93-1.02	0.31
Tumor size	1.26	0.66-2.41	0.49
Nodal status	3.18	2.22-4.56	<0.001
Tumor grade	0.67	0.41-1.09	0.11
ER	0.85	0.57-1.27	0.42
PgR	0.74	0.55-0.1	0.05
Treatment arm	0.82	0.42-1.59	0.55
Phospho-S6RP	0.70	0.29-1.69	0.42

Table 26: Multivariate Cox proportional hazards model.

*95% CI = 95% confidence interval.

Variables were coded as described in Table 14

.

3.4.4 Predictive analysis of phospho-S6RP:

The interaction of phospho-S6RP and extended adjuvant treatment was evaluated in a Cox model that included age, tumor size, nodal status, tumor grade, ER expression, PgR expression, treatment arm, phospho-S6RP expression, and an interaction term, the product of phospho-S6RP and treatment arm. In this model the interaction term was not significant (P=0.76) and, therefore, phospho-S6RP has no predictive value in our study population (Table 27).

Variable	**Hazard ratio for distant recurrence**	**95% CI***	**P**
Age	0.98	0.93-1.02	0.31
Tumor size	1.26	0.66-2.42	0.48
Nodal status	3.2	2.22-4.6	<0.001
Tumor grade	0.67	0.41-1.09	0.11
ER	0.85	0.57-1.27	0.42
PgR	0.75	0.56-1.0	0.05
Treatment arm	0.85	0.42-1.75	0.67
Phospho-S6RP	1.04	0.07-14.79	0.98
Phospho-S6RP x treatment arm	0.75	0.12-4.80	0.76

Table 27: Interaction analysis.
*95% CI = 95% confidence interval.
Variables were coded as described in Table 14.

3.5 Predictive analysis of clinicopathological parameters in the ABCSG 6a study population:

Finally, we studied the interaction between clinicopathological parameters and extended adjuvant endocrine therapy in the ABCSG 6a patient population. This analysis was performed

in the total ABCSG 6a study population (n=856). Again multivariate Cox models that included age, tumor size, nodal status, tumor grade, ER expression, PgR expression, treatment arm, and an interaction term, were used. The interaction terms are shown in Table 28. A significant interaction was observed between high PgR expression and extended adjuvant endocrine treatment (P<0.001). The scoring of hormone-receptor status (ER and PgR) used in this study is based on the semi-quantitative Reiner score [64] and was classified as negative, low, medium, high. If we investigated the treatment benefit according to the different PgR categories, we observed that the benefit of extended adjuvant endocrine therapy significantly increased with increasing PgR-positivity. Figure 18 shows the impact of the two treatment arms (no further treatment or 3 years of anastrazole) on DRFS for each PgR expression category. Thus, women with high PgR expression appear to benefit from extension of endocrine therapy after 5 years of treatment with tamoxifen (P=0.001), whereas patients with low or medium PgR expression do not (P=0.80 and P=0.25, respectively) (figures 18b-d). Moreover, patients with negative PgR expression status have a significantly shorter DRFS if they received extended adjuvant endocrine therapy (P=0.016) (figure 18a). Therefore, according to these results, only women with high PgR expression in their tumors should be treated with extended adjuvant endocrine therapy.

Interaction term	**Interaction P**
Treatment arm x age	0.76
Treatment arm x tumor size	0.64
Treatment arm x nodal status	0.53
Treatment arm x tumor grade	0.35
Treatment arm x ER	0.12
Treatment arm x PgR	<0.001

Table 28: Interaction analysis. All interaction P values were derived from single multivariate Cox models (data not shown).

(a)

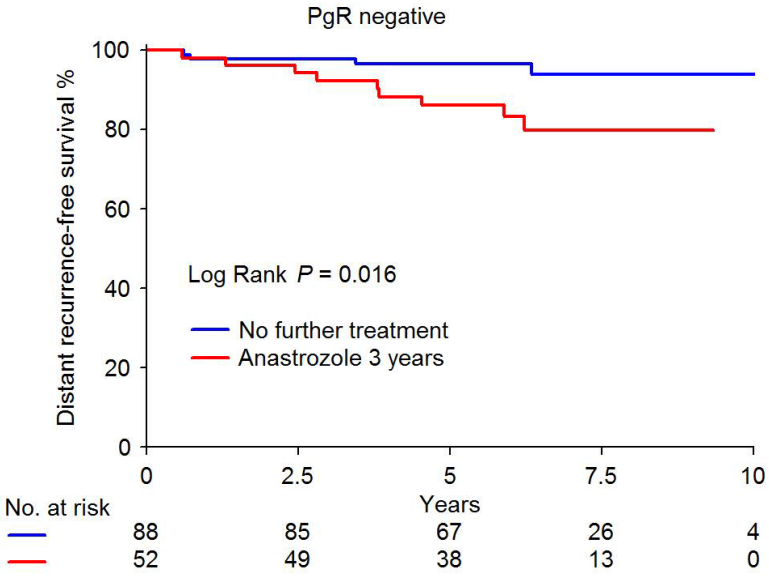
PgR negative
Distant recurrence-free survival %
100
80
60
40
20
0
Log Rank P = 0.016
No further treatment
Anastrozole 3 years
0
2.5
5
7.5
10
Years
No. at risk
88
85
67
26
4
52
49
38
13
0

(b)

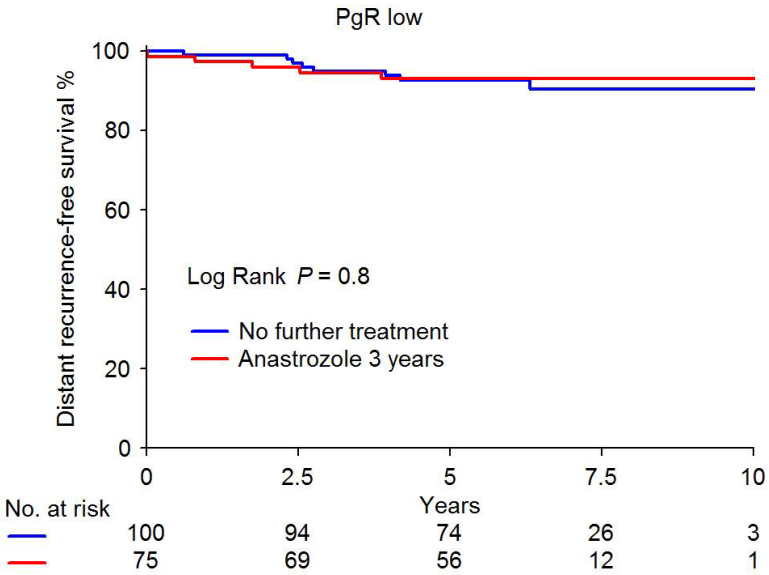
PgR low
Distant recurrence-free survival %
100
80
60
40
20
0
Log Rank P = 0.8
No further treatment
Anastrozole 3 years
0
2.5
5
7.5
10
Years
No. at risk
100
94
74
26
3
75
69
56
12
1

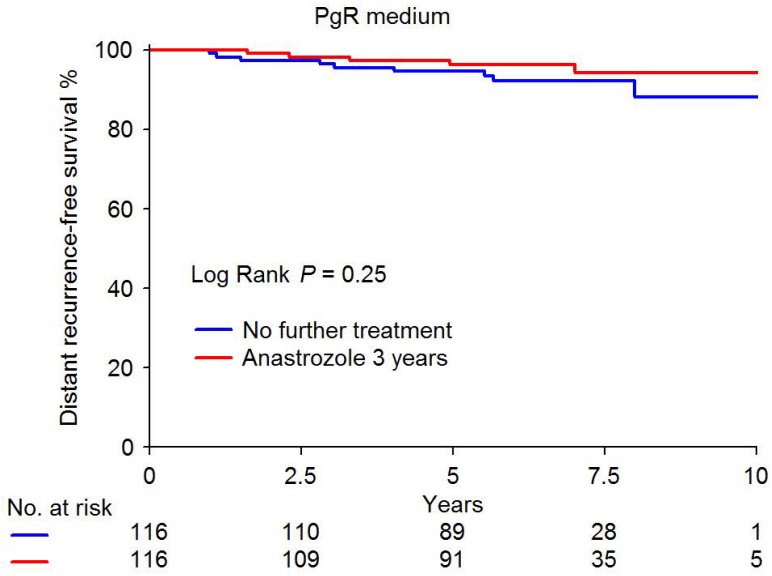

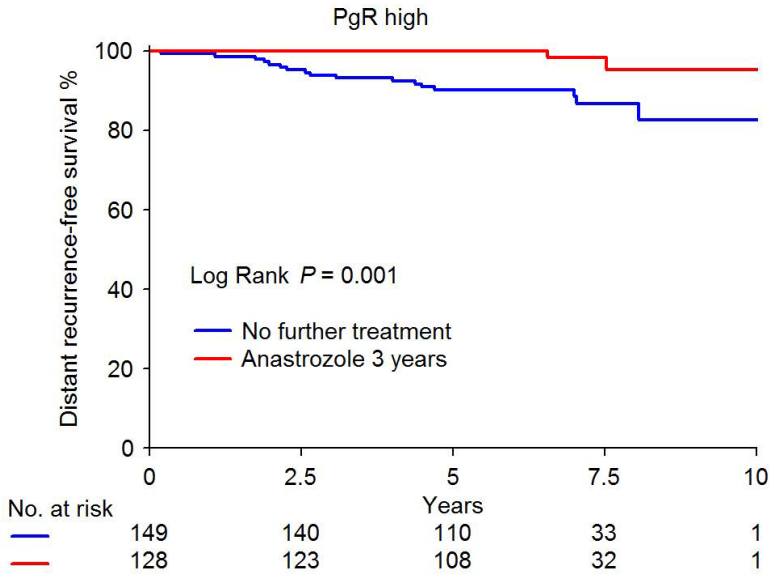

Figure 18: Kaplan-Meier plots of DRFS according to ABCSG 6a treatment arms (no further treatment or 3 years of anastrazole) in patients with (a) negative, (b) low, (c) medium, (d) or high PgR expression status.

Discussion

In the present study, *PIK3CA* mutational status, phospho-mTOR expression, phospho-S6RP expression and clinicopathological parameters were analyzed with regard to their potential prognostic and/or predictive value in a large cohort of postmenopausal, endocrine-responsive breast cancer patients.
Mutation analysis of the *PIK3CA* gene revealed a mutation rate of 42.4% in ER-positive breast cancer patients who were treated within the randomized trial ABCSG 6a. This mutation frequency confirms the results of a recent study by Sabine et al. (2014) analyzing patients from the TEAM trial. This study reported a *PIK3CA* mutation rate of 40% in a large study cohort of more than 4000 patients. Additionally the Genome Cancer Atlas Network (2012) indicated *PIK3CA* as the most common significantly mutated gene (SMG) in luminal A breast cancer and reported a mutation frequency of 45%.

PIK3CA mutations were assessed by pyrosequencing. This enzymatic method quantifies inorganic pyrophosphate released at each sequence elongation step by proportionally converting it into visible light. In contrast to Sanger sequencing no modified or fluorescently labeled nucleotides are required neither to stop DNA elongation nor for the later readout of the synthesized sequence. Instead specific dispensing cycles allow the addition of only one type of dNTP at a time which induces a light reaction if matching the complementary strand. Each light emission generates a peak in a pyrogram. No chain-termination, such as for Sanger sequencing is required and therefore low-quality regions (10-40 bases), due to primer annealing at the beginning of each newly synthesized DNA strand, can be avoided.
Major advantages of this pyrosequencing method also include a relatively fast run-time (17-50 minutes, depending on the assay) in combination with a relatively high throughput (processing of 24 samples simultaneously). The pyrosequencing technology allows sequencing of a mixture of DNA molecules (different DNA templates) which are amplified separately and thereby cloning can be avoided.
The principal limitation of this method is its restriction to a short accurate read length of approximately 80-220 base pairs. In contrast, the Sanger method allows sequencing of reads with a length of up to 1 kb of base pairs.
For the present study, which aimed to detect hot spot mutations that cluster in short, specific domains of the *PIK3CA* gene and in which high mutation frequencies were already reported, the pyrosequencing technology is particularly useful [8] [62]. Pyrosequencing also allows precise quantification of allele or SNP variants [65].Various studies for the detection of KRAS mutations showed that a higher sensitivity could be achieved with Pyrosequencing

compared to Sanger sequencing [65][66]. The limit of detection for Pyrosequencing is approximately 5% of mutated alleles whereas for Sanger sequencing it is already reached at 15 to 20% [66].
Overall, the pyrosequencing allows precise and high-throughput analysis of breast tumor samples and even enabled the detection of various so far unknown point mutations in the *PIK3CA* gene.

It is well known that mutations in certain genes function as drivers of cancer and promote therapy resistance. However, in our study we demonstrated that mutations in the *PIK3CA* gene were not associated with outcome particularly DRFS and, therefore, is no prognostic marker. In addition, recurrence-free survival (RFS) was determined as a second endpoint for comparison. For RFS also invasive ipsilateral breast tumor recurrence and local or regional recurrence in addition to distant recurrence is defined as endpoint event. Using RFS as endpoint for survival analysis we confirmed that *PIK3CA* mutational status had no prognostic value.
In our study, we observed no correlations between the mutational status of *PIK3CA* and other tumor and patients characteristics. In contrast to these results, Sabine et al. (2014) found correlations of *PIK3CA* mutations with various favorable prognostic factors such as, low tumor grade or absence of lymph node involvement.

Most importantly and in contrast to all previous studies, the predictive value of *PIK3CA* mutational status for treatment response was investigated. Analysis of interaction between treatment arms of ABCSG 6a and mutational status failed to demonstrate significant effects on DRFS. Similar results were observed if RFS was used as an endpoint of the survival analysis. However as the annual breast cancer specific mortality rate for ER-positive breast cancer does not decrease after 5-10 years after diagnosis and treatment, definitive conclusions require a longer follow-up time. Thus, patient follow-up data will be updated in the next years to test potential long term effects of the impact of *PIK3CA* mutations on adjuvant endocrine treatment.

Another aim of this study was to gain deeper insights into the clinical relevance of downstream effectors of the PI3-kinase pathway by analysis of immunohistochemical staining of whole tumor tissue sections of tumor blocks from ABCSG 6a patients. As the

PI3K/Akt/mTOR pathway is frequently deregulated in breast cancer and other tumor types it would provide a promising target for anti-tumor therapy.

mTOR is a central regulator of gene translation and important for cellular metabolism and consequently proliferation and growth. It is a major downstream protein of the PI3-kinase pathway which is frequently deregulated or overexpressed and is also involved in treatment resistance.

The development of resistance against anti-estrogen therapy can result from estrogen-independent phosphorylation of estrogen receptor alpha at the activation-function domain 1 (AF-1) specifically at Ser167. In vitro studies demonstrated that a crosstalk between the mTORC1/S6K1 pathway and estrogen independent signaling via phosphorylation of Ser167 exists [67]. An improvement in clinical outcome was achieved for ER-positive postmenopausal patients by administration of the mTOR inhibitor everolimus ancillary to endocrine therapy in the context of the BOLERO-2 study, a Phase III clinical trial [68].

Immunohistochemical analyses in the context of this study aimed to demonstrate the presence of phospho-mTOR and one of its principal downstream targets, S6 ribosomal protein, in order to draw conclusions about their relationship in the context of breast cancer and to analyze direct consequences and impacts of these components of the PI3K-signaling cascade on patient prognosis and therapy outcomes.

According to the literature in invasive breast cancer the phosphorylated and consequently activated form of phospho-mTOR was associated with a threefold increased risk for cancer relapse. Overexpression of the protein was reported for 24% of invasive breast tumors [69].

In our study, immunohistochemical staining of phospho-mTOR revealed that 61% of tumor tissue samples had low phospho-mTOR status while the remaining 49% were classified as high. A prognostic value of phospho-mTOR with regard to DRFS could not be shown for ER-positive postmenopausal women. Additional statistical analysis with RFS as study endpoint revealed no impact of phospho-mTOR on cancer recurrences. There may be several reasons for this discrepancy. As the cut-off was set relatively low a large proportion of patients were graded as highly positive for phospho-mTOR. Additionally classification of phospho-mTOR-expression in the study of Bose et al. (2006) was based on a different scoring scheme and the study was not restricted to ER-positive breast cancer which could also explain differences in results as well.

However a significant interaction of phospho-mTOR with adjuvant treatment was demonstrated thus suggesting mTOR in its phosphorylated form as a predictive marker for extended adjuvant endocrine therapy. Kaplan Meier curves in patients with low phospho-

mTOR expression in their tumors indicate no difference between the two treatment arms of ABCSG 6a. Among patients featuring high phosphor-mTOR expression a significantly longer DRFS was observed in the extended adjuvant endocrine treatment arm compared to no further treatment. Although patients of the ABCSG 6a trial were not treated with mTOR inhibitors this study demonstrates that further depletion of estrogen after 5 years of tamoxifen which competes with estrogen for binding to ER, may be essential for some patients. Administration of the aromatase inhibitor anastrazole for additional three years was successful in minimizing long-term risks in patients of high phospho-mTOR status. Thus, after careful validation of our results in independent studies, the determination of phospho-mTOR expression as predictive marker would offer a more precise application of endocrine therapy by the identification of patients facing increased risk of relapse after standard endocrine treatment.

To further analyze the PI3-kinase pathway downstream of mTOR, we performed immunohistochemical staining for S6 ribosomal protein.
Although it was expected that samples featuring phospho-mTOR exhibit similar staining scores for phosphor-S6 ribosomal protein statistical analysis did not provide evidence for a correlation between these proteins. In addition, no prognostic and/or predictive value of phospho-S6RP could be demonstrated. In contrast, the tissue-array based analysis of breast tumor samples of Bose et al. (2006) showed a weak correlation between phospho-S6RP and phospho-mTOR. However, overexpression of pS6RP in 72% of tumor samples also lay far above the rate of overexpressed phospho-mTOR (24%).
A comparison of phospho-S6RP with characteristics of patients of ABCSG 6a revealed no correlation of pS6RP-status with age of the patient, tumor size, lymph node status, tumor grade, or the presence of estrogen or progesterone receptors. Absence of these correlations was also shown in microarray studies in which FISH was used to analyze pS6 amplification in breast tumor tissue [70].
Although a significant correlation of phospho-S6RP with the proliferation marker Ki-67 was shown, no association of phospho-S6RP with distant cancer recurrence and death from breast cancer was revealed. However phospho-S6RP as a part of the 40S ribosomal subunit is required especially in translation of components of the ribosomal machinery itself which is in turn required for cell growth, especially during fast proliferation. High Ki-67 and consequently high cellular proliferation requires high efficiency of translation by implicating phospho-S6RP and subsequent generation of new ribosomes for the maintenance and regeneration of the enzymatic setting of cells.

Broader understanding of basic molecular mechanisms that escape translational control in cancer and which could therefore provide novel targets for anticancer therapy still need to be identified. Furthermore the identification of specific molecular signatures could reveal new prognostic or therapeutic markers that allow a more precise evaluation of patient prognosis and therapeutic needs.
In addition to S6RP, S6 kinase 1 or 4E-BP1 are important factors of the PI3K/Akt/mTOR pathway. In order to get a more complete picture on the impact of mTOR on disease development and progression an analysis of these proteins may be necessary. Overexpression of the translational repressor protein 4E-BP1 in its phosphorylated and consequently inactive stage was observed in over 59% of breast tumors (n=103) in a study from Rojo et al. [71]. In this study, phospho-4E-BP1 is significantly correlated with tumor size and the presence of positive lymph nodes and was detected in increased levels in case of locoregional recurrence of patients.

In our study, we were able to investigate the predictive value of clinicopathological variables of ABCSG 6a patients including hormone receptor expression. ER-positive patients feature different levels of PgR or can even be progesterone negative. The prognostic value of PgR was confirmed in various clinical trials showing a longer disease-free survival for patients whose breast tumors express higher levels of PgR [72]. In addition, the presence of PgR was important for the outcome of endocrine therapy as the risk reduction was higher for ER-positive/PgR-positive patients compared to ER-positive/PgR-negative patients [73].
Analyses of patients from ABCSG 6a revealed that PgR is an independent predictive marker for the extension of endocrine therapy. We demonstrated that patients with high PgR expression have a decreased risk to develop distant metastases if extended endocrine therapy with anastrazole was administered. Similar results were obtained if RFS was used as study endpoint. In conclusion, our data suggest that extension of the standard endocrine treatment of 5 years of tamoxifen with the aromatase inhibitor anastrazole for further three years is particularly beneficial in patients with high PgR.
It would be interesting to confirm our findings in breast cancer patients who received other aromatase inhibitors such as letrozole as extended adjuvant therapy [74]. However, no results comparing letrozole benefit in context to PgR-status of patients are currently available.
In conclusion**,** we demonstrated that *PIK3CA* mutations had no significant prognostic and/or predictive relevance in a large cohort of breast cancer patients. Most importantly, we showed that women with high phospho-mTOR expression or high PgR expression appear to benefit

from extension of endocrine therapy after 5 years of treatment with tamoxifen, whereas patients with low phospho-mTOR expression or low PgR expression do not. If these results could be confirmed in other studies these markers can be easily implemented in clinical routine and may help to select postmenopausal, hormone receptor-positive breast cancer patients for extended adjuvant endocrine treatment.

References:

[1] P. Taneja, D. Maglic, F. Kai, S. Zhu, R. D. Kendig, E. A. Fry, and K. Inoue, "Classical and Novel Prognostic Markers for Breast Cancer and their Clinical Significance.," *Clin. Med. Insights. Oncol.*, vol. 4, pp. 15–34, Jan. 2010.

[2] J. a Engelman, J. Luo, and L. C. Cantley, "The evolution of phosphatidylinositol 3-kinases as regulators of growth and metabolism.," *Nat. Rev. Genet.*, vol. 7, no. 8, pp. 606–19, Aug. 2006.

[3] L. M. Amzel, C. Huang, D. Mandelker, C. Lengauer, S. B. Gabelli, and B. Vogelstein, "NIH Public Access," vol. 8, no. 9, pp. 665–669, 2010.

[4] D. a Fruman, R. E. Meyers, and L. C. Cantley, "Phosphoinositide kinases.," *Annu. Rev. Biochem.*, vol. 67, pp. 481–507, Jan. 1998.

[5] D. Stokoe, L. R. Stephens, T. Copeland, P. R. J. Gaffney, C. B. Reese, G. F. Painter, A. B. Holmes, F. Mccormick, and P. T. Hawkins, "Dual Role of Phosphatidylinositol-3 , 4 , 5- trisphosphate in the Activation of Protein Kinase B," pp. 2–6, 1997.

[6] K. E. Bachman, P. Argani, Y. Samuels, N. Silliman, J. Ptak, S. Szabo, H. Konishi, B. Karakas, B. G. Blair, C. Lin, B. A. Peters, V. E. Velculescu, and B. H. Park, "The PIK3CA Gene is Mutated with High Frequency Bio sci No t D ist r ibu te," vol. 3, no. 8, pp. 772–775, 2004.

[7] Cancer Genome Atlas Network, "Comrehensive molecular portraits of human breast tumors," *Nature*, vol. 490, no. 7418, pp. 61–70, 2012.

[8] V. S. Sabine, C. Crozier, C. L. Brookes, C. Drake, T. Piper, C. J. H. van de Velde, A. Hasenburg, D. G. Kieback, C. Markopoulos, L. Dirix, C. Seynaeve, D. W. Rea, and J. M. S. Bartlett, "Mutational analysis of PI3K/AKT signaling pathway in tamoxifen exemestane adjuvant multinational pathology study.," *J. Clin. Oncol.*, vol. 32, no. 27, pp. 2951–8, Sep. 2014.

[9] M. Gymnopoulos, M.-A. Elsliger, and P. K. Vogt, "Rare cancer-specific mutations in PIK3CA show gain of function.," *Proc. Natl. Acad. Sci. U. S. A.*, vol. 104, no. 13, pp. 5569–74, Mar. 2007.

[10] S. Kang, A. G. Bader, and P. K. Vogt, "Phosphatidylinositol 3-kinase mutations identified in human cancer are oncogenic.," *Proc. Natl. Acad. Sci. U. S. A.*, vol. 102, no. 3, pp. 802–7, Jan. 2005.

[11] A. G. Dumont, S. N. Dumont, and J. C. Trent, "The favorable impact of PIK3CA mutations on survival: an analysis of 2587 patients with breast cancer," pp. 327–334, 2012.

[12] C. K. Lee, C. Brown, R. J. Gralla, V. Hirsh, S. Thongprasert, C.-M. Tsai, E. H. Tan, J. C.-M. Ho, D. T. Chu, A. Zaatar, J. A. Osorio Sanchez, V. Van Vu, J. S. K. Au, A. Inoue, S. M. Lee, V. Gebski, and J. C.-H. Yang, "Impact of EGFR inhibitor in non-

small cell lung cancer on progression-free and overall survival: a meta-analysis.," *J. Natl. Cancer Inst.*, vol. 105, no. 9, pp. 595–605, May 2013.

[13] R. A. Campbell, P. Bhat-Nakshatri, N. M. Patel, D. Constantinidou, S. Ali, and H. Nakshatri, "Phosphatidylinositol 3-kinase/AKT-mediated activation of estrogen receptor alpha: a new model for anti-estrogen resistance.," *J. Biol. Chem.*, vol. 276, no. 13, pp. 9817–24, Mar. 2001.

[14] T. W. Miller, J. M. Balko, and C. L. Arteaga, "Phosphatidylinositol 3-kinase and antiestrogen resistance in breast cancer.," *J. Clin. Oncol.*, vol. 29, no. 33, pp. 4452–61, Nov. 2011.

[15] J. Shou, S. Massarweh, C. K. Osborne, a. E. Wakeling, S. Ali, H. Weiss, and R. Schiff, "Mechanisms of Tamoxifen Resistance: Increased Estrogen Receptor-HER2/neu Cross-Talk in ER/HER2-Positive Breast Cancer," *JNCI J. Natl. Cancer Inst.*, vol. 96, no. 12, pp. 926–935, Jun. 2004.

[16] T. W. Grunt and G. L. Mariani, "Novel Approaches for Molecular Targeted Therapy of Breast Cancer: Interfering with PI3K/AKT/mTOR Signaling," *Curr. Cancer Drug Targets*, vol. 13, no. 2, pp. 188–204, Mar. 2013.

[17] B. Alberts, A. Johnson, J. Lewis, M. Raff, K. Roberts, and P. Walter, "Molecular Biology of the Cell." Garland Science, 2007.

[18] G. Song, G. Ouyang, and S. Bao, "The activation of Akt / PKB signaling pathway and cell survival," vol. 9, no. 1, pp. 59–71, 2005.

[19] R. C. Hresko and M. Mueckler, "mTOR??RICTOR is the Ser473 kinase for Akt/protein kinase B in 3T3-L1 adipocytes," *J. Biol. Chem.*, vol. 280, no. 49, pp. 40406–40416, Dec. 2005.

[20] E. Jacinto, V. Facchinetti, D. Liu, N. Soto, S. Wei, S. Y. Jung, Q. Huang, J. Qin, and B. Su, "SIN1/MIP1 maintains rictor-mTOR complex integrity and regulates Akt phosphorylation and substrate specificity.," *Cell*, vol. 127, no. 1, pp. 125–37, Oct. 2006.

[21] A. C. Gingras, S. G. Kennedy, M. a. O'Leary, N. Sonenberg, and N. Hay, "4E-BP1, a repressor of mRNA translation, is phosphorylated and inactivated by the Akt(PKB) signaling pathway," *Genes Dev.*, vol. 12, no. 4, pp. 502–513, 1998.

[22] A. Alayev and M. K. Holz, "mTOR signaling for biological control and cancer.," *J. Cell. Physiol.*, vol. 228, no. 8, pp. 1658–64, Aug. 2013.

[23] F. Meric-Bernstam and A. M. Gonzalez-Angulo, "Targeting the mTOR signaling network for cancer therapy.," *J. Clin. Oncol.*, vol. 27, no. 13, pp. 2278–87, May 2009.

[24] K. Inoki, Y. Li, T. Zhu, J. Wu, and K.-L. Guan, "TSC2 is phosphorylated and inhibited by Akt and suppresses mTOR signalling.," *Nat. Cell Biol.*, vol. 4, no. 9, pp. 648–657, Sep. 2002.

[25] J. Kunz, R. Henriquez, U. Schneider, M. Deuter-Reinhard, N. R. Movva, and M. N. Hall, “Target of rapamycin in yeast, TOR2, is an essential phosphatidylinositol kinase homolog required for G1 progression.,” *Cell*, vol. 73, no. 3, pp. 585–96, May 1993.

[26] D. M. Sabatini, H. Erdjument-bromage, M. Lui, P. Tempst, and S. H. Snyder, “RAFTI□: A Mammalian Protein That Binds to FKBP12 in a Rapamycin-Dependent Fashion and Is Homologous to Yeast TORs,” vol. 78, pp. 35–43, 1994.

[27] E. Brown, M. Albers, T. Shin, K. Ichikawa, C. Keith, W. Lane, and S. Schreiber, “A mammalian protein targeted by G1-arresting rapamycin-receptor complex,” *Nature*, vol. 369, no. 6483, pp. 756–8, 1994.

[28] M. Laplante and D. M. Sabatini, “mTOR signaling at a glance.,” *J. Cell Sci.*, vol. 122, no. Pt 20, pp. 3589–94, Oct. 2009.

[29] K. Hara, Y. Maruki, X. Long, K. Yoshino, N. Oshiro, S. Hidayat, C. Tokunaga, J. Avruch, and K. Yonezawa, “Raptor, a Binding Partner of Target of Rapamycin (TOR), Mediates TOR Action,” *Cell*, vol. 110, no. 2, pp. 177–189, Jul. 2002.

[30] N. Oshiro, R. Takahashi, K. Yoshino, K. Tanimura, A. Nakashima, S. Eguchi, T. Miyamoto, K. Hara, K. Takehana, J. Avruch, U. Kikkawa, and K. Yonezawa, “The proline-rich Akt substrate of 40 kDa (PRAS40) is a physiological substrate of mammalian target of rapamycin complex 1.,” *J. Biol. Chem.*, vol. 282, no. 28, pp. 20329–39, Jul. 2007.

[31] Y. Sancak, C. C. Thoreen, T. R. Peterson, R. a Lindquist, S. a Kang, E. Spooner, S. a Carr, and D. M. Sabatini, “PRAS40 is an insulin-regulated inhibitor of the mTORC1 protein kinase.,” *Mol. Cell*, vol. 25, no. 6, pp. 903–15, Mar. 2007.

[32] L. Wang, T. E. Harris, R. a Roth, and J. C. Lawrence, “PRAS40 regulates mTORC1 kinase activity by functioning as a direct inhibitor of substrate binding.,” *J. Biol. Chem.*, vol. 282, no. 27, pp. 20036–44, Jul. 2007.

[33] T. R. Peterson, M. Laplante, C. C. Thoreen, Y. Sancak, S. A. Kang, W. M. Kuehl, N. S. Gray, and D. M. Sabatini, “NIH Public Access,” vol. 137, no. 5, pp. 873–886, 2010.

[34] D. a Guertin, D. M. Stevens, C. C. Thoreen, A. a Burds, N. Y. Kalaany, J. Moffat, M. Brown, K. J. Fitzgerald, and D. M. Sabatini, “Ablation in mice of the mTORC components raptor, rictor, or mLST8 reveals that mTORC2 is required for signaling to Akt-FOXO and PKCalpha, but not S6K1.,” *Dev. Cell*, vol. 11, no. 6, pp. 859–71, Dec. 2006.

[35] D. D. Sarbassov, S. M. Ali, D.-H. Kim, D. a Guertin, R. R. Latek, H. Erdjument-Bromage, P. Tempst, and D. M. Sabatini, “Rictor, a novel binding partner of mTOR, defines a rapamycin-insensitive and raptor-independent pathway that regulates the cytoskeleton.,” *Curr. Biol.*, vol. 14, no. 14, pp. 1296–302, Jul. 2004.

[36] D. D. Sarbassov, D. A. Guertin, and S. M. Ali, “Phosphorylation and Regulation of Akt / PKB by the Rictor-mTOR Complex,” vol. 307, no. December 2004, pp. 1098–1102, 2005.

[37] M. a Frias, C. C. Thoreen, J. D. Jaffe, W. Schroder, T. Sculley, S. a Carr, and D. M. Sabatini, “mSin1 is necessary for Akt/PKB phosphorylation, and its isoforms define three distinct mTORC2s.,” *Curr. Biol.*, vol. 16, no. 18, pp. 1865–70, Sep. 2006.

[38] Y. Mamane, E. Petroulakis, O. LeBacquer, and N. Sonenberg, “mTOR, translation initiation and cancer.,” *Oncogene*, vol. 25, no. 48, pp. 6416–22, Oct. 2006.

[39] N. Hay and N. Sonenberg, “Upstream and downstream of mTOR,” pp. 1926–1945, 2004.

[40] G. J. Brunn, C. C. Hudson, A. Sekulic, J. M. Williams, H. Hosoi, P. J. Houghton, J. C. L. Jr, and R. T. Abraham, “Phosphorylation of the Translational Repressor PHAS-I by the Mammalian Target of Rapamycin,” 1997.

[41] P. E. Burnett, R. K. Barrow, N. A. Cohen, S. H. Snyder, and D. M. Sabatini, “RAFT1 phosphorylation of the translational regulators p70 S6 kinase and 4E-BP1.,” *Proc. Natl. Acad. Sci. U. S. A.*, vol. 95, no. 4, pp. 1432–7, Feb. 1998.

[42] a.-C. Gingras, S. P. Gygi, B. Raught, R. D. Polakiewicz, R. T. Abraham, M. F. Hoekstra, R. Aebersold, and N. Sonenberg, “Regulation of 4E-BP1 phosphorylation: a novel two-step mechanism,” *Genes Dev.*, vol. 13, no. 11, pp. 1422–1437, Jun. 1999.

[43] A. Gingras, B. Raught, S. P. Gygi, A. Niedzwiecka, M. Miron, S. K. Burley, R. D. Polakiewicz, A. Wyslouch-cieszynska, R. Aebersold, and N. Sonenberg, “Hierarchical phosphorylation of the translation inhibitor 4E-BP1,” pp. 2852–2864, 2001.

[44] K. A. Martin and J. Blenis, “of Translation by the PI 3-Kinase and mTOR Pathways REGULATORY PATHWAYS,” 2002.

[45] O. Meyuhas, “Synthesis of the translational apparatus is regulated at the translational level,” *Eur. J. Biochem.*, vol. 267, no. 21, pp. 6321–6330, Nov. 2000.

[46] M. Pende, S. H. Um, V. Mieulet, M. Sticker, V. L. Goss, J. Mestan, M. Mueller, S. Fumagalli, S. C. Kozma, and G. Thomas, “S6K1-/-/S6K2-/- Mice Exhibit Perinatal Lethality and Rapamycin-Sensitive 5 J -Terminal Oligopyrimidine mRNA Translation and Reveal a Mitogen-Activated Protein Kinase-Dependent S6 Kinase Pathway,” vol. 24, no. 8, pp. 3112–3124, 2004.

[47] a Goldhirsch, E. P. Winer, a S. Coates, R. D. Gelber, M. Piccart-Gebhart, B. Thürlimann, and H.-J. Senn, “Personalizing the treatment of women with early breast cancer: highlights of the St Gallen International Expert Consensus on the Primary Therapy of Early Breast Cancer 2013.,” *Ann. Oncol.*, vol. 24, no. 9, pp. 2206–23, Sep. 2013.

[48] C. M. Perou, T. Sùrlie, M. B. Eisen, M. Van De Rijn, S. S. Jeffrey, C. A. Rees, J. R. Pollack, D. T. Ross, H. Johnsen, L. A. Akslen, I. Fluge, A. Pergamenschikov, C. Williams, S. X. Zhu, P. E. Lùnning, P. O. Brown, D. Botstein, and S. Grant, “Molecular portraits of human breast tumours,” vol. 533, no. May, pp. 747–752, 2000.

[49] T. Sørlie, C. M. Perou, R. Tibshirani, T. Aas, S. Geisler, H. Johnsen, T. Hastie, M. B. Eisen, M. Van De Rijn, S. S. Jeffrey, T. Thorsen, H. Quist, J. C. Matese, P. O. Brown,

D. Botstein, P. Eystein, and A. Børresen-dale, “Gene expression patterns of breast carcinomas distinguish tumor subclasses with clinical implications,” vol. 98, no. 19, 2001.

[50] “Hormone therapy for breast cancer.” [Online]. Available: http://www.cancer.org/cancer/breastcancer/detailedguide/breast-cancer-treating-hormone-therapy. [Accessed: 05-Feb-2015].

[51] A. A. Thike, P. Y. Cheok, A. R. Jara-Lazaro, B. Tan, P. Tan, and P. H. Tan, “Triple-negative breast cancer: clinicopathological characteristics and relationship with basal-like breast cancer.,” *Mod. Pathol.*, vol. 23, no. 1, pp. 123–33, Jan. 2010.

[52] T. Sørlie, R. Tibshirani, J. Parker, T. Hastie, J. S. Marron, A. Nobel, S. Deng, H. Johnsen, R. Pesich, S. Geisler, J. Demeter, C. M. Perou, P. E. Lønning, P. O. Brown, and D. Botstein, “Repeated observation of breast tumor subtypes in independent gene expression data sets,” vol. 100, no. 14, pp. 8418–8423, 2003.

[53] a García Fernández, C. Chabrera, M. García Font, M. Fraile, J. M. Lain, S. Gónzalez, I. Barco, C. González, J. Torres, M. Piqueras, L. Cirera, E. Veloso, a Pessarrodona, and N. Giménez, “Differential patterns of recurrence and specific survival between luminal A and luminal B breast cancer according to recent changes in the 2013 St Gallen immunohistochemical classification.,” *Clin. Transl. Oncol.*, Oct. 2014.

[54] C. Davies, J. Godwin, R. Gray, M. Clarke, D. Cutter, S. Darby, P. McGale, H. C. Pan, C. Taylor, Y. C. Wang, M. Dowsett, J. Ingle, and R. Peto, “Relevance of breast cancer hormone receptors and other factors to the efficacy of adjuvant tamoxifen: patient-level meta-analysis of randomised trials.,” *Lancet*, vol. 378, no. 9793, pp. 771–84, Aug. 2011.

[55] B. L. Riggs and L. C. Hartmann, “030213 Selective Estrogen-Receptor Modulators — Mechanisms of Action,” vol. 348, no. 12, 2014.

[56] K. Mokbel, “The evolving role of aromatase inhibitors in breast cancer,” pp. 279–283, 2002.

[57] K.-D. Yu, J. Wu, Z.-Z. Shen, and Z.-M. Shao, “Hazard of breast cancer-specific mortality among women with estrogen receptor-positive breast cancer after five years from diagnosis: implication for extended endocrine therapy.,” *J. Clin. Endocrinol. Metab.*, vol. 97, no. 12, pp. E2201–9, Dec. 2012.

[58] R. Jakesz, R. Greil, M. Gnant, M. Schmid, W. Kwasny, E. Kubista, B. Mlineritsch, C. Tausch, M. Stierer, F. Hofbauer, K. Renner, C. Dadak, E. Rücklinger, and H. Samonigg, “Extended adjuvant therapy with anastrozole among postmenopausal breast cancer patients: results from the randomized Austrian Breast and Colorectal Cancer Study Group Trial 6a.,” *J. Natl. Cancer Inst.*, vol. 99, no. 24, pp. 1845–53, Dec. 2007.

[59] W. Jonat, M. Gnant, F. Boccardo, M. Kaufmann, A. Rubagotti, I. Zuna, M. Greenwood, and R. Jakesz, “Effectiveness of switching from adjuvant tamoxifen to anastrozole in postmenopausal women with hormone-sensitive early-stage breast cancer: a meta-analysis.,” *Lancet. Oncol.*, vol. 7, no. 12, pp. 991–6, Dec. 2006.

[60] M. Knauer, M. Filipits, and P. Dubsky, “Late Recurrences in Early Breast Cancer: For Whom and How Long Is Endocrine Therapy Beneficial?,” *Breast Care*, vol. 8, pp. 97–100, 2014.

[61] M. Schmid, “Randomized Trial of Tamoxifen Versus Tamoxifen Plus Aminoglutethimide as Adjuvant Treatment in Postmenopausal Breast Cancer Patients With Hormone Receptor-Positive Disease: Austrian Breast and Colorectal Cancer Study Group Trial 6,” *J. Clin. Oncol.*, vol. 21, no. 6, pp. 984–990, Mar. 2003.

[62] K. Nosho, T. Kawasaki, M. Ohnishi, Y. Suemoto, G. J. Kirkner, D. Zepf, Y. Liying, J. A. Longtine, C. S. Fuchs, and S. Ogino, “PIK3CA Mutation in Colorectal Cancer : Relationship with Genetic,” vol. 10, no. 6, pp. 534–541, 2008.

[63] C. A. Hudis, W. E. Barlow, J. P. Costantino, R. J. Gray, K. I. Pritchard, J.-A. W. Chapman, J. A. Sparano, S. Hunsberger, R. a Enos, R. D. Gelber, and J. A. Zujewski, “Proposal for standardized definitions for efficacy end points in adjuvant breast cancer trials: the STEEP system.,” *J. Clin. Oncol.*, vol. 25, no. 15, pp. 2127–32, May 2007.

[64] P. Regitnig, A. Reiner, H.-P. Dinges, G. Höfler, E. Müller-Holzner, S. F. Lax, P. Obrist, M. Rudas, and F. Quehenberger, “Quality assurance for detection of estrogen and progesterone receptors by immunohistochemistry in Austrian pathology laboratories.,” *Virchows Arch.*, vol. 441, no. 4, pp. 328–34, Oct. 2002.

[65] S. Ogino, T. Kawasaki, M. Brahmandam, L. Yan, M. Cantor, C. Namgyal, M. Mino-Kenudson, G. Y. Lauwers, M. Loda, and C. S. Fuchs, “Sensitive sequencing method for KRAS mutation detection by Pyrosequencing.,” *J. Mol. Diagn.*, vol. 7, no. 3, pp. 413–21, Aug. 2005.

[66] A. C. Tsiatis, A. Norris-Kirby, R. G. Rich, M. J. Hafez, C. D. Gocke, J. R. Eshleman, and K. M. Murphy, “Comparison of Sanger sequencing, pyrosequencing, and melting curve analysis for the detection of KRAS mutations: diagnostic and clinical implications.,” *J. Mol. Diagn.*, vol. 12, no. 4, pp. 425–32, Jul. 2010.

[67] R. L. Yamnik and M. K. Holz, “mTOR/S6K1 and MAPK/RSK signaling pathways coordinately regulate estrogen receptor alpha serine 167 phosphorylation.,” *FEBS Lett.*, vol. 584, no. 1, pp. 124–8, Jan. 2010.

[68] K. I. Pritchard, F. Lebrun, J. T. Beck, Y. Ito, D. Yardley, I. Deleu, A. Perez, T. Bachelot, D. Ph, L. Vittori, M. Sc, Z. Xu, P. Mukhopadhyay, and D. Lebwohl, “Everolimus in Postmenopausal Hormone- Receptor–Positive Advanced Breast Cancer,” 2012.

[69] S. Bose, S. Chandran, J. M. Mirocha, and N. Bose, “The Akt pathway in human breast cancer: a tissue-array-based analysis.,” *Mod. Pathol.*, vol. 19, no. 2, pp. 238–45, Mar. 2006.

[70] M. Ba, J. Kononen, L. Bubendorf, Y. Chen, M. L. Bittner, J. Torhorst, P. Haas, C. Bucher, G. Sauter, and O. Kallioniemi, “Detecting Activation of Ribosomal S6 Kinase by Complementary DNA and Tissue Microarray Analysis,” vol. 92, no. 15, pp. 2–9, 2000.

[71] F. Rojo, L. Najera, J. Lirola, J. Jiménez, M. Guzmán, M. D. Sabadell, J. Baselga, and S. Ramon y Cajal, "4E-binding protein 1, a cell signaling hallmark in breast cancer that correlates with pathologic grade and prognosis.," *Clin. Cancer Res.*, vol. 13, no. 1, pp. 81–9, Jan. 2007.

[72] W. L. Mcguire, G. M. Clark, and D. Ph, "Role of Progesterone Receptors In Breast Cancer."

[73] V.-J. Bardou, G. Arpino, R. M. Elledge, C. K. Osborne, and G. M. Clark, "Progesterone receptor status significantly improves outcome prediction over estrogen receptor status alone for adjuvant endocrine therapy in two large breast cancer databases.," *J. Clin. Oncol.*, vol. 21, no. 10, pp. 1973–9, May 2003.

[74] P. E. Goss, J. N. Ingle, S. Martino, N. J. Robert, H. B. Muss, M. J. Piccart, M. Castiglione, D. Tu, L. E. Shepherd, K. I. Pritchard, R. B. Livingston, N. E. Davidson, L. Norton, E. a Perez, J. S. Abrams, D. a Cameron, M. J. Palmer, and J. L. Pater, "Randomized trial of letrozole following tamoxifen as extended adjuvant therapy in receptor-positive breast cancer: updated findings from NCIC CTG MA.17.," *J. Natl. Cancer Inst.*, vol. 97, no. 17, pp. 1262–71, Sep. 2005.

List of figures:

List of tables:

Danksagung

Ich möchte an dieser Stelle meinen Dank an all jene, die mich während meiner Masterarbeit begleitet und motiviert haben zum Ausdruck bringen.

Zu aller erst danke ich meinem Betreuer und Projektleiter Assoc. Prof. Mag. Dr. Filipits für das Bereitstellen dieses interessanten Themas für meine Masterarbeit und für seine verlässliche Unterstützung und Rückhalt während des gesamten Arbeitsverlaufes bis hin zur Korrektur der geschriebenen Arbeit.

Großer Dank gilt auch meiner Betreuerin Anita Brandstetter welche sehr viel Zeit aufgewendet hat um mich sorgfältig in alle mir neuen Techniken einzuschulen, mir wertvolle Tipps gegeben hat und auf deren Hilfestellung, auch als freundschaftliche Ansprechpartnerin ich mich immer verlassen konnte.

Ich danke auch meinen Kollegen am Institut, die mich so oft aufgeheiterte und ermutigt haben.

Außerdem gilt ein besonderer Dank meiner Familie, insbesondere meinen Eltern die mir dieses Studium ermöglicht und mir Selbstvertrauen gegeben haben und mir in dieser Zeit eine unglaubliche seelische und moralische Stütze waren.

Nicht zuletzt möchte ich mich bei meinem Freund Owen bedanken der mir nicht nur linguistisch bei der Verfassung der Arbeit zur Seite stand, sondern dessen Zuwendung und Verständnis mir in den letzten Monaten sehr geholfen hat.

Curriculum vitae

Personal data:

Name: Anna Buder
Nationality: Austria

Education:

Since May 2014: Master thesis at the Institute of Cancer Research of the Medical University of Vienna in the research group of Prof. Filipits

Summer term 2013: Exchange term at the Université Paul-Sabatier in Toulouse (France)

Since 2012: Master study in "Molecular Microbiology & Immunobiology"

2009-2012: Bachelor study in Biology at the University of Vienna

2001-2009: Modern language grammar school "Kreuzschwestern" in Linz

1997-2001: Elementary school "Kreuzschwestern" in Linz